



Cite this: *Nanoscale*, 2023, **15**, 19016

## Progress in the design of portable colorimetric chemical sensing devices

Tushar Kant, <sup>\*a</sup> Kamlesh Shrivastava, <sup>\*b</sup> Ankita Tejwani, <sup>b</sup> Khushali Tandey, <sup>b</sup> Anuradha Sharma<sup>c</sup> and Shashi Gupta<sup>c</sup>

The need for precise determination of heavy metals, anions, biomolecules, pesticides, drugs, and other substances is vital across clinical, environmental, and food safety domains. Recent years have seen significant progress in portable colorimetric chemical sensing devices, revolutionizing on-the-spot analysis. This review offers a comprehensive overview of these advancements, covering handheld colorimetry, RGB-based colorimetry, paper-based colorimetry, and wearable colorimetry devices. It explores the underlying principles, functional materials (chromophoric reagents/dyes and nanoparticles), detection mechanisms, and their applications in environmental monitoring, clinical care, and food safety. Noble metal nanoparticles (NPs) have arisen as promising substitutes in the realm of sensing materials. They display notable advantages, including heightened sensitivity, the ability to fine-tune their plasmonic characteristics for improved selectivity, and the capacity to induce visible color changes, and simplifying detection. Integration of NPs fabricated paper device with smartphones and wearables facilitates reagent-free, cost-effective, and portable colorimetric sensing, enabling real-time analysis and remote monitoring.

Received 31st July 2023,

Accepted 27th October 2023

DOI: 10.1039/d3nr03803c

rsc.li/nanoscale

### 1. Introduction

The determination of heavy metals, biomolecules, pesticides, volatile organic compounds (VOCs), drugs, and several other materials plays a vital role in clinical, environmental, and food safety applications. In clinical backgrounds, the exact exposure of biomolecules, such as proteins and genetic markers, is vital for diagnosing diseases, monitoring treatment efficacy, and ensuring optimal patient care. Environmental monitoring relies on the analysis of heavy metals and VOCs to assess pollution levels, identify sources of contamination, and protect ecosystems and human health. Pesticide analysis is essential in agricultural practices to ensure safe and sustainable food production while minimizing environmental impact. Additionally, in food safety, the identification of contaminants and nutrients is critical for ensuring the quality and safety of food products and safeguarding consumers' well-being. Overall, precise determination of these substances in different contexts is indispensable for public health protection, environmental

preservation, and maintaining high food safety standards.<sup>1–5</sup>

Numerous analytical methods are utilized in diverse applications for identification and examination of metals, biomolecules, toxicants, and various other substances. For metal detection, methods such as atomic absorption spectroscopy (AAS),<sup>6</sup> inductively coupled plasma-atomic emission spectroscopy (ICP-AES),<sup>7</sup> ICP-mass spectrometry (MS),<sup>8</sup> fluorimetry,<sup>9</sup> and electroanalytical methods<sup>10</sup> are commonly utilized. In the analysis of biomolecules, pesticides, drugs, and volatile organic compounds (VOCs) from environmental, clinical, food, and industrial samples, techniques like fluorimetry,<sup>11</sup> electroanalytical methods,<sup>12</sup> high-performance liquid chromatography (HPLC),<sup>13</sup> gas chromatography (GC),<sup>14</sup> liquid chromatography-mass spectrometry (LC-MS),<sup>15</sup> and gas chromatography-mass spectrometry (GC-MS)<sup>16</sup> are widely used. The selection of specific methods depends on the nature of the substances being analyzed, the desired level of sensitivity and accuracy, and the particular application requirements. AAS, ICP-AES, ICP-MS, GC, HPLC, GC-MS, LC-MS, fluorimetry, and electroanalytical methods exhibit high sensitivity for detecting various chemical substances; however, they can be expensive, require trained personnel, and may not be applicable at the sample sources.

Among the analytical methods discussed, colorimetry, often referred to as spectrophotometry, distinguishes itself as a straightforward and easily accessible approach for identify-

<sup>a</sup>Shaheed Kawasi Rodda Pedda, Govt. College Kuakonda, Dantewada-494552, CG, India. E-mail: tusharkant40@gmail.com

<sup>b</sup>School of Studies in Chemistry, Pt. Ravishankar Shukla University, Raipur-492010, CG, India. E-mail: kshrivastava@gmail.com

<sup>c</sup>Department of Zoology, Govt. Nagarjuna P.G. College of Science, Raipur-492010, CG, India

ing a wide range of chemical compounds. The fundamental principle of colorimetry centers around the quantitative analysis of chemical substances in a solution. This analysis is achieved by measuring the absorption of light, which occurs when colored complexes are formed through a chemical reaction between chromophoric reagents or dyes and the target analyte.<sup>17–20</sup> Indeed, this method have its drawbacks. One major limitation is the necessity for specific chromophoric reagents or dyes tailored to the target analyte, which can be time-consuming and expensive to develop or acquire. Moreover, the relatively large volume of solution required (approximately 3–5 mL) adds to the overall cost of the analysis. Furthermore, it is possible to encounter selectivity challenges, which can create difficulties in accurately differentiating the desired analyte from other substances within the solution. These considerations highlight the need for alternative analytical approaches that can overcome these limitations and provide more cost-effective and selective measurements.<sup>21,22</sup>

Noble metal nanoparticles (NPs) such as gold (Au), silver (Ag) and copper have gained significant attention as colorimetric sensing probes in place of traditional chromophoric reagents or dyes. These NPs exhibit exceptional sensitivity due to their strong localized surface plasmon resonances (LSPR), allowing for the detection of minute concentrations of analytes with high precision. The tunable plasmonic properties of noble metal NPs enable tailoring their sensing capabilities to specific analytes, enhancing selectivity. Their color changes are visually detectable, obviating the need for complex instrumentation and making colorimetric sensing accessible in various settings. Moreover, the stability and photostability of noble metal NPs ensure reliable and reproducible results over time.<sup>23–26</sup> Their biocompatibility, particularly in the case of Au and AgNPs, expands their utility to biomedical applications. Surface functionalization facilitates the development of targeted and specific sensing platforms, while the cost-effectiveness of synthesis methods allows for mass production and practical implementation. This reagent-free and cost-effective nature of NP-based colorimetric sensing makes it a promising and versatile tool for the detection of a variety of chemical substances.

Smartphone and wearable colorimetric detection refers to the use of smartphones or wearable devices to perform color-based analyses for detecting and measuring chemical substances in various applications. Smartphones and wearable electronics now come with high-resolution cameras and powerful image processing tools because of advances in technology. It now becomes possible to use these gadgets as easily transportable and available equipment for colorimetric analysis. Images of the reaction mixture or sample are often taken, and then using specialized software or mobile applications, the color changes are analyzed and turned into quantitative data.<sup>27–30</sup> The integration of colorimetric detection with smartphones and wearables offers several advantages. Firstly, it eliminates the need for bulky and expensive laboratory equipment, making it more cost-effective and accessible, particularly in resource-limited settings or for on-the-spot testing.

Additionally, it allows for real-time analysis and remote monitoring, enabling rapid response and data sharing. Smartphone and wearable colorimetric detection finds applications across diverse domains, encompassing medical diagnostics (such as the identification of biomarkers for diseases), environmental surveillance (like assessing water quality), ensuring food safety (including the detection of contaminants), and various other areas. As technology continues to advance, the potential for these devices to revolutionize on-the-go colorimetric detection and data collection is promising. However, it is essential to address challenges such as calibration, accuracy, and standardization to ensure reliable and precise results.<sup>31–36</sup>

In conclusion, this review provides details on how the addition of NPs, chromophores, and probes has increased the sensor capacity for the determination of chemical substances. This review article provides explanation of improvements in portable colorimetric chemical sensing devices. It also details how the research combination of paper-based sensor systems, smartphone compatibility, and portable techniques have all deeply changed the field of chemical sensing. They hold great potential for various uses, such as environmental surveillance, industrial applications and point-of-care medical testing since these portable sensors associate these various technologies to give rapid sensitive and inexpensive detection methods. For scientists and engineers who are interested in the most recent developments in this field, this review will be a great resource.

## 2. Principle for sensing of chemical substances using portable colorimetry

### 2.1. Handheld colorimetry devices

A portable handheld colorimetric device is a compact, user-friendly tool used for analyzing the concentration of specific substances in a sample based on color changes. It operates on the principle of colorimetry, measuring the light absorption or transmission at a particular wavelength. To use the device, the sample solution with chromophoric reagents or metal NPs is placed onto the testing platform. These reagents/NPs initiate a chemical reaction with the sample, leading to color changes. The device then detects and quantifies the color changes, which are directly proportional to the concentration of the substance being analyzed.<sup>37</sup> These devices are commonly used in various fields, including environmental monitoring, water quality testing, medical diagnostics, and food safety assessments. Portable handheld colorimetric devices offer several advantages, such as rapid analysis, minimal sample preparation, and ease of use in the field or remote locations. Due to their compact size, they are highly convenient for on-site measurements and can be easily carried around by researchers, technicians, or field operators. The devices come with pre-calibrated settings for specific substances, ensuring accurate and reliable measurements.<sup>38,39</sup> Fig. 1 illustrates the graphical scheme of a portable colorimetric device where the concentration of a chemical substance in an unknown sample solution can be directly monitored from the sample sites.

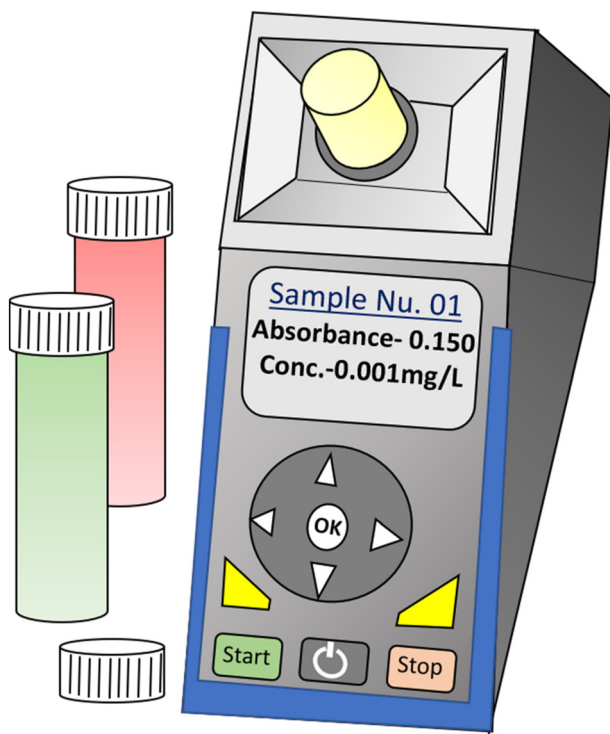


**Fig. 1** A portable handheld colorimetry device for the self-referenced solution-based determination of the analyte.

## 2.2. RGB-based colorimetry

Red green and blue (RGB)-based portable colorimetry is a color measurement technique used to analyze the color of samples in various applications. A portable colorimeter utilizes a light source consisting of light-emitting diodes (LEDs)

to illuminate the sample. Sensors are then used to capture the intensity of the red, green, and blue light components from the reflected light. Each sensor provides numerical RGB values corresponding to the sample's color. The RGB values obtained are typically converted to a standard color space to enable accurate color representation and comparison across different devices and systems.<sup>40,41</sup> A portable handheld RGB-based colorimetric device for self-referenced solution-based determination of the analyte is shown in Fig. 2 (a–c). This method is particularly useful in industries like food, textiles, cosmetics, and printing, where consistent and precise color matching is essential. RGB-based portable colorimeters are user-friendly and suitable for on-site measurements, making them ideal for quality control and color assessment in manufacturing or field applications. Due to their compact size and ease of use, these devices are commonly utilized in mobile or remote locations requiring immediate color analysis. Calibration procedure ensure the accuracy and reliability of color measurements, allowing for consistent and repeatable results. The device's display often provides color difference values, allowing users to assess how closely the sample matches a specified color standard.<sup>42,43</sup> With advancements in technology, some RGB-based colorimeters may also have wireless connectivity options, enabling data transfer and remote monitoring. Overall, RGB-based portable colorimetry offers a convenient and efficient solution for quick and accurate color analysis in a variety of industries and settings.

## 2.3. RGB paper-based colorimetry

RGB paper-based colorimetry is a cutting-edge method that leverages the ubiquity and capabilities of smartphones for color analysis on paper test strips. The test strips are designed

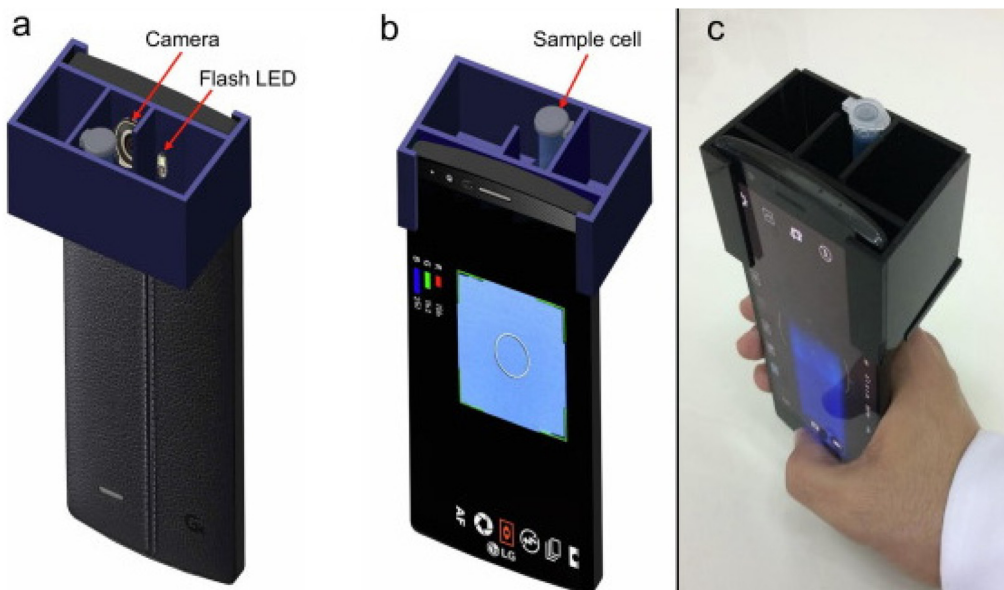


**Fig. 2** (a–c) show the portable handheld RGB-based colorimetry device for the self-referenced solution-based determination of the water content in ethanol [this figure has been reproduced from ref. 40 with permission from Elsevier Sciences, copyright 2020].

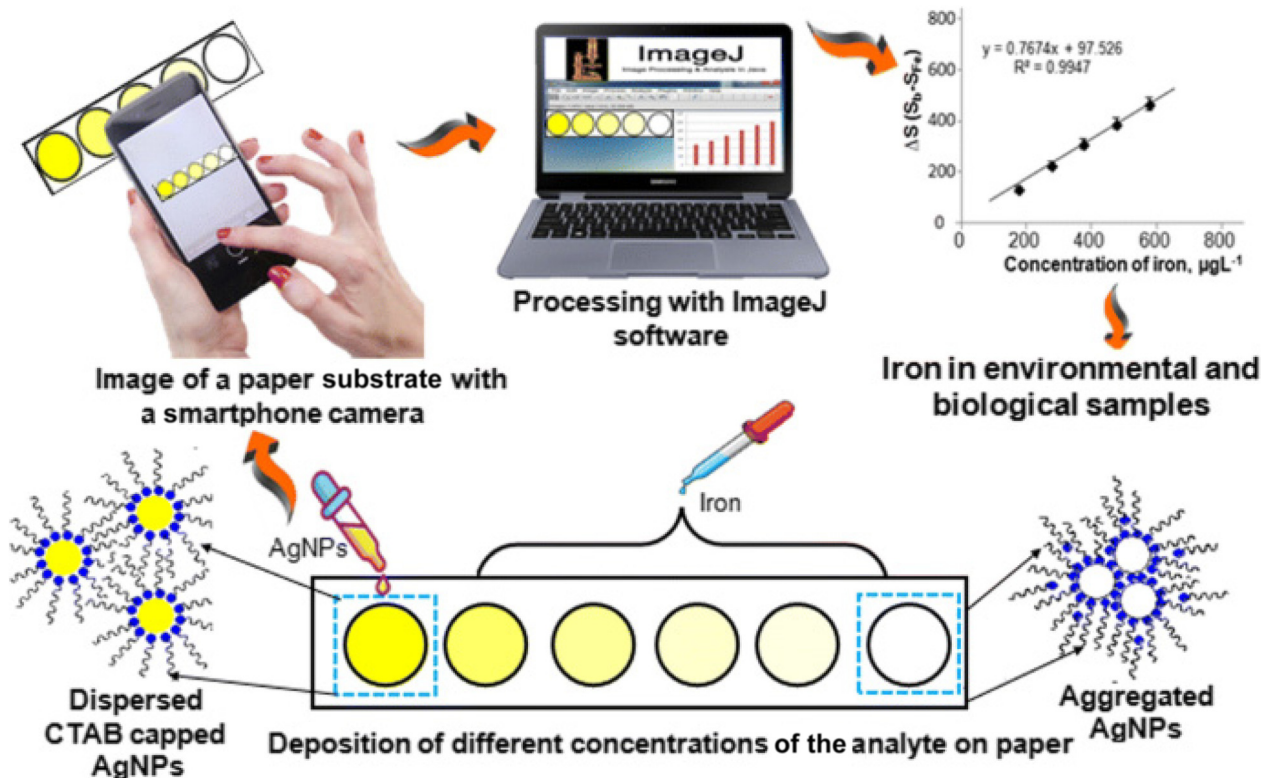


**Fig. 3** Design and development of a smartphone-assisted paper-based portable colorimetric device for the on-site detection of the analyte [this figure has been reproduced from ref. 44 with permission from Springer Nature, copyright 2020].

with specific reagents that cause a visible color change upon interaction with the target analyte. To perform the colorimetric measurement, the user places the test strip onto a flat surface and launches the designated colorimetry app on their smartphone. The smartphone's camera captures an image of the test strip, and the app extracts the RGB color values from the image, representing the intensity of red, green, and blue light. These RGB values are then converted into a measurable color parameter, such as absorbance or concentration, using calibration curves or algorithms embedded in the app. The colorimetric data can be instantly displayed on the smartphone's screen, providing real-time analysis and results. The design and development of a smartphone-assisted paper-based portable colorimetric device for on-site detection of the analyte is shown in Fig. 3. Generally, this method is particularly advantageous for point-of-care testing, environmental monitoring, and resource-limited settings where traditional laboratory equipment may not be readily available. The smartphone-based approach offers portability, cost-effectiveness, and ease of use, making it accessible to a wide range of users, including researchers, healthcare professionals, and even the general public. The paper-based nature of the test strips also enables easy and low-cost manufacturing, making it feasible for mass production and distribution. Furthermore, the integration of smartphone technology allows for data sharing, remote monitoring, and potential integration with cloud-based databases for broader data analysis and trend tracking.<sup>44–46</sup> Overall, RGB-

based smartphone paper-based colorimetry opens up exciting possibilities for democratizing colorimetric analysis and expanding its applications to various fields and scenarios.

### 3. Functional materials and mechanism for selective detection

Portable colorimetric sensors have mainly been used for on-site analysis due to their portability and easy handling. These sensors offer increased sensitivity and selectivity by including a variety of advanced materials, like various metallic NPs, chromophores, and dyes. Complex instrumentation is not required in this system because it provides visible color changes in response to analyte detection.

#### 3.1. Chromophoric reagents and organic dyes used as molecular sensing probes

Molecular sensing probes rely on chromophoric reagents and organic dyes to respond optically to specific target molecules. By incorporating recognition elements, these probes can selectively interact with their intended targets, leading to changes in the chromophore's properties. These alterations in the optical signals are measured using techniques such as UV-Vis spectroscopy, fluorescence spectroscopy, or colorimetric assays. Additionally, their optical readouts offer real-time and non-destructive measurements, rendering them appropriate

for a wide range of medical applications, environmental and analytical fields. For example, Ren *et al.*<sup>47</sup> designed an azo-benzene-based 4'-hydroxyl-2,4-diaminoazobenzene (HDAB) sensing probe for  $\text{Al}^{3+}$  and  $\text{Fe}^{3+}$  detection using a smartphone. When HDAB was introduced to the solution of metal ions such as  $\text{Al}^{3+}$  and  $\text{Fe}^{3+}$ , it resulted in the formation of a 1:1 complex, causing a noticeable shift in color from yellow to purple and a corresponding increase in the absorption band. Herein,  $\text{Al}^{3+}$  and  $\text{Fe}^{3+}$  ions (2.0 mM–20 M) in water samples were colorimetrically detected using test paper coated with a multifunctional probe and utilized in conjunction with a smartphone for both visual inspection and digital image colorimetry. Ranbir and coworkers<sup>48</sup> demonstrated a cellulose paper-based sensor strip for colorimetric monitoring of biogenic amines. These amines are released during the decarboxylation of amino acids, a process that occurs while packing protein-based nutritional products. Herein, a paper sensor strip was prepared using different metal ion-based chromophores (azo-dyes), which show photophysical properties to confirm colorimetric response in the presence of amines. As the azo dye undergoes a structural change upon binding to the target biogenic amine, it results in a noticeable color change in the sensor. This is a potential approach for the identification of biogenic amines in food safety monitoring.

Vellingiri *et al.*<sup>49</sup> demonstrated the identification of nitrite ions ( $\text{NO}_2^-$ ) in water and wastewater by employing fuchsin dye as a colorimetric indicator. They applied basic fuchsin (BF) onto Whatman filter paper, and observed that when  $\text{NO}_2^-$  ions at various concentrations ranging from 0.005 to 9.2 mg  $\text{L}^{-1}$  were introduced to the BF-coated paper, a noticeable color transition from pink to colorless ensued as a result of diazotization. This color change offered a visible indication of the presence of  $\text{NO}_2^-$  ions. The LOD value was calculated to be 0.005 mg  $\text{L}^{-1}$  and the change in color intensity was measured, and the calculated RGB value using an RGB analyzer which is shown in Fig. 4 corresponded to the concentration of the

analyte present in the sample. Chen and group<sup>50</sup> presented a colorimetric sensing probe using Nile red, zinc tetraphenyl porphyrin (Zn-TPP), and methyl red dyes to monitor the aging and spoilage of chicken at different temperatures. The sensing principle relies on the reaction of these dyes with the emanating gas released from chicken meat. The sensor was constructed with vapor-sensitive dyes enclosed in resin microbeads, arranged in a barcode sequence on an affordable paper substrate. Each barcode pattern exhibits distinct colors, and the RGB values of these patterns can be calculated using a smartphone.

Liu and coworkers<sup>51</sup> demonstrated a paper sensor based on a dye/dye-Cu-MOF (metal–organic framework) for detecting mildewed wheat. Four dyes, namely bromocresol purple, bromophenol blue, bromophenol red, and bromoxylenol blue, were employed to prepare the dye/dye-Cu-MOF complex. When mildewed wheat is introduced into a sealed container, it emits a variety of volatile gases that result in the deprotonation of phenolic hydroxyl groups. The existence of bromine atoms speeds up the process of electron extraction, and the addition of  $\text{Cu}^{2+}$  has the potential to give rise to ion associates. The color change of the sensor depends on whether the dyes gain or lose electrons, and the RGB values are analyzed accordingly.

Despite their advantages, molecular sensing probes using chromophoric reagents and organic dyes may have intrinsic drawbacks such as photobleaching susceptibility, low stability, and possible toxicity. Additionally, the design and synthesis of highly specific probes can be challenging and may require extensive optimization for different target molecules. On the other hand, because of their distinct features, NPs provide a convincing substitute as probes for portable colorimetric sensing applications. Nanomaterials overcome the drawbacks of conventional chromophores and dyes with their enhanced sensitivity, excellent stability, and adjustable properties. They are also perfect for mobile and field-based sensing applications because of their tiny size, which makes it simple to integrate them into portable equipment.

### 3.2. Nanomaterials used as colorimetric sensing probes

Stability, size-dependent color variations, and plasmonic effects are crucial for portable colorimetric sensing. These characteristics make nanomaterials like silver nanoparticles (AgNPs), gold nanoparticles (AuNPs), copper nanoparticles (CuNPs), graphene, and quantum dots (QDs) appropriate for portable colorimetric sensing probes.

**3.2.1. AuNPs.** The unique characteristics of AuNPs make them ideal as portable colorimetric sensors. They are excellent materials for portable and user-friendly colorimetric sensors due to their stability, biocompatibility, and simplicity of production. Various methods have been documented for the synthesis of AuNPs, including the chemical reduction process, green synthesis, and sono-chemical processes. However, the chemical reduction process is particularly prevalent because of its straightforward and uncomplicated nature.<sup>52</sup>

For example, Cho *et al.*<sup>53</sup> reported a portable colorimetric sensing method utilizing AuNPs as a sensing probe to detect

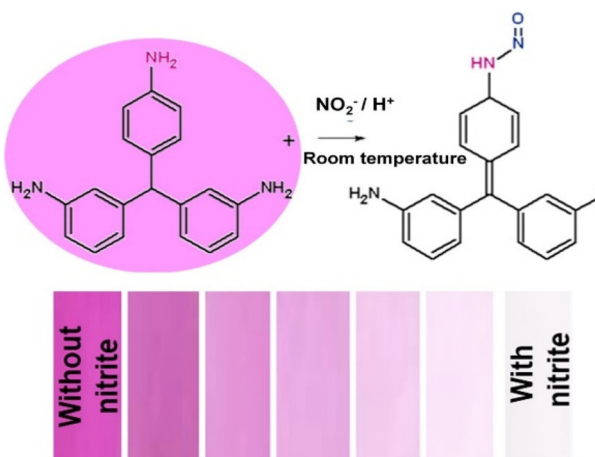


Fig. 4 Systematic representation of fuchsin dye-based nitrite ion ( $\text{NO}_2^-$ ) detection in real water and wastewater samples [this figure has been reproduced from ref. 49 with permission from Elsevier Sciences, copyright 2019].

$\text{Cd}^{2+}$  in potable water samples. The study involved the synthesis of glutathione-functionalized AuNPs (AuNPs-GSH) through a citrate reduction approach, which were then deposited on a flexible polyethylene terephthalate (PET) substrate using polyvinyl pyrrolidone (PVP) as a binder. The study demonstrated that AuNPs-GSH exhibited aggregation in aqueous environments upon exposure to  $\text{Cd}^{2+}$ , resulting in a distinct visual transformation of the solution color from red to blue. The aggregation is facilitated by the chelation of  $\text{Cd}^{2+}$  ions to the glutamyl amino groups of GSH anchored onto the surface of AuNPs. In another example, Zhang and coworkers<sup>54</sup> developed a synthesis process to prepare vinyl phosphonic acid (VPA) functionalized AuNPs with a distinctive wine-red color using the  $\text{NaBH}_4$  reduction method. They established a smartphone-based colorimetric sensing technique to detect uranyl ions ( $\text{UO}_2^{2+}$ ) in water samples. When AuNPs-VPA were introduced to the  $\text{UO}_2^{2+}$  sample, the AuNPs underwent a color shift, transitioning from a wine-red shade to blue, and the smartphone application 'photo-matrix' measured the intensity of this color change. This method allowed for the determination of  $\text{UO}_2^{2+}$  at a minimum concentration of 2  $\mu\text{M}$ .

Duenchay *et al.*<sup>55</sup> developed flexible sensing strips for the detection of vitamin B1 in urine samples. They achieved this by depositing AuNPs on a transparency sheet. AuNPs were synthesized using a citrate reduction method without the need for further modifications and were stabilized by the negatively charged citrate ions. The principle for estimating the vitamin B1 concentration is based on the aggregation of AuNPs, which occurs as a result of electrostatic interactions between vitamin B1, carrying a positive charge, and citrate ions with a negative charge, responsible for stabilizing the AuNPs. As a consequence, this led to a noticeable color change in the transparency paper sheet, which was then processed using the ImageJ application on a smartphone to generate RGB colors for quantitative measurement of B1 in urine samples.

Gan and coworkers<sup>56</sup> developed an on-site colorimetric detection method for  $\text{Cd}^{2+}$  in water, employing aptamer-functionalized AuNPs (AuNPs-aptamer) as a sensing probe. The researchers utilized a self-developed smartphone-based application to optimize the color change in the solution. In this approach, the stability of AuNPs-aptamer in the presence of NaCl can be attributed to the repulsion between the negatively charged aptamers coating the NPs, which prevents their self-aggregation. However, upon the addition of  $\text{Cd}^{2+}$  to the AuNPs-aptamer solution, the aptamer exhibited a higher affinity for  $\text{Cd}^{2+}$ , resulting in self-elimination from the AuNPs. The color of the solution was changed, and the procedure and mechanism are shown in Fig. 5. An image processing software was used for the extraction RGB intensity of the paper substrate for quantitative estimation of the target substance. The LOD value calculated for  $\text{Cd}^{2+}$  was 1.12  $\mu\text{g L}^{-1}$  in the water sample, which is less than the permissible limit (5  $\mu\text{g L}^{-1}$ ) of  $\text{Cd}^{2+}$  in drinking water.

Esfahani and group<sup>57</sup> presented an innovative technique for quantifying phosphate ( $\text{PO}_4^{3-}$ ) ions through the use of a stable  $\text{Eu}^{3+}$  tablet-based method, in which AuNPs stabilized

with mercaptoacetic acid (MAA) played a pivotal role. In this method,  $\text{Eu}^{3+}$  is encapsulated within a dextran matrix, forming a tablet-shaped structure. Subsequently, this dextran-encapsulated  $\text{Eu}^{3+}$  tablet was dissolved in the water sample intended for analysis, and AuNPs-MAA was introduced. As a result of this process, a distinctive color shift, transitioning from blue to red, was observed. This transformation occurred due to the surface plasmon resonance (SPR) effect, brought about by the aggregation of AuNPs in the presence of  $\text{PO}_4^{3-}$ . Rajamanikandan *et al.*<sup>58</sup> introduced a fast, straightforward, and user-friendly approach for the sensitive detection of cysteine (Cys) by utilizing AuNPs functionalized with  $\beta$ -cyclodextrin ( $\beta$ -CD). The high binding affinity of Cys's thiol group to the surface of AuNPs- $\beta$ -CD, leading to the formation of Au-thiol bonds, resulted in aggregation and observable colorimetric changes.

Thus, AuNPs serve as effective tools for portable colorimetric sensing, offering stability and ease of production. They are utilized in various studies for rapid and user-friendly detection of substances, although the cost of synthesizing AuNPs remains a limiting factor. Nevertheless, AuNP-based sensors hold promise for point-of-care diagnostics and environmental monitoring, with ongoing efforts to address associated challenges.

**3.2.2 AgNPs.** AgNP-based portable colorimetric sensors have several advantages. They first provide sensitive and speedy analyte detection, enabling on-site testing and real-time monitoring. Second, these sensors are practical for point-of-care diagnostics in environments with limited resources because they are inexpensive than AuNPs and easy to use.<sup>59</sup> Furthermore, AgNPs exhibit high levels of stability, ensuring reproducible results. The portability of these sensors also allows for field testing and remote monitoring. AgNPs are an environmentally friendly alternative to other metal NPs, making them a viable option for the development of sensors. AgNPs are also stable in nature like AuNPs and they can be synthesized by various methods like chemical reduction, green synthesis, hydrothermal and electrochemical methods, *etc.*

For example, Monisha and coworkers<sup>60</sup> proposed a chemical reduction method to prepare AgNPs for the detection of  $\text{Hg}^{2+}$ . The researchers utilized  $\text{NaBH}_4$  and PVP as the reducing and capping agents, respectively, leading to the synthesis of PVP-capped AgNPs. These NPs were printed on filter paper using the inkjet printing method. Subsequently, when  $\text{Hg}^{2+}$  solution was dropped onto the printed paper substrate and allowed to stand for a few min, a transition in color from yellow to colorless took place, and the alteration in color intensity was quantified using ImageJ software on a smartphone. The approach for the synthesis of AgNPs-PVP and the mechanism for colorimetric detection of  $\text{Hg}^{2+}$  are shown in Fig. 6 (a-f).

Shrivastava *et al.*<sup>44</sup> introduced an innovative technique for synthesizing AgNPs to facilitate on-site detection of  $\text{Fe}^{3+}$  in both biological and environmental samples. Different capping agents, such as bare AgNPs, AgNPs-CTAB, AgNPs-CPC, and AgNPs-citrate, were utilized for AgNP synthesis, among which

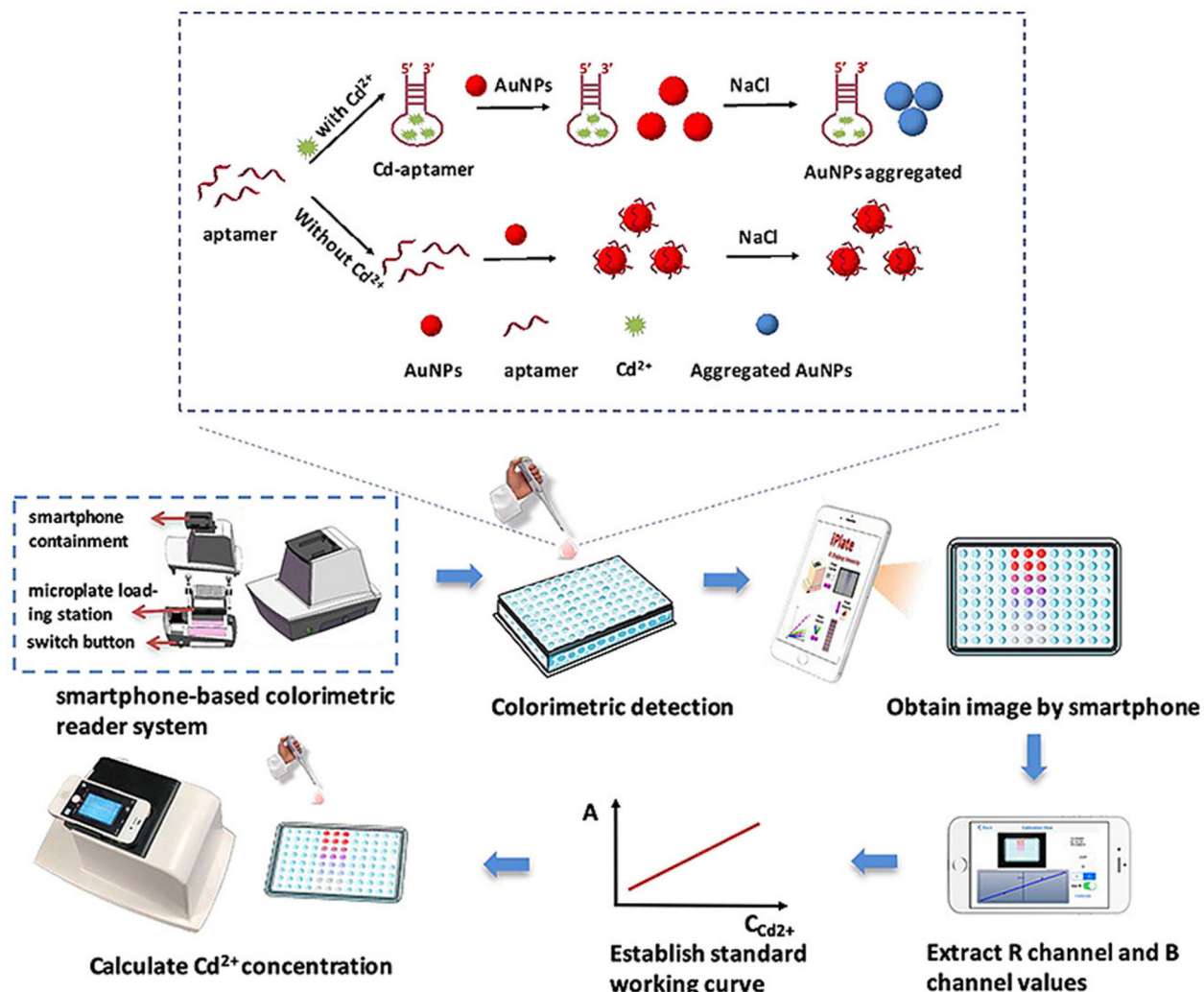


**Fig. 5** Mechanism of the detection of  $\text{Cd}^{2+}$  in drinking water using an AuNP-aptamer based sensing probe [this figure has been reproduced from ref. 56 with permission from Elsevier Sciences, copyright 2020].

citrate capped NPs were found to be suitable for the detection of  $\text{Fe}^{3+}$ . The NPs impregnated on paper showed yellow color and the introduction of  $\text{Fe}^{3+}$  resulted in discoloration due to the aggregation of AgNPs. This approach exhibited a favorable relative recovery range of 91.3%–95.0% and showcased its capability for the selective determination of total iron in both water and blood plasma samples, as confirmed by interference studies.

Another work by Shrivastava and colleagues<sup>61</sup> presented a study showcasing AgNP-based paper analytical devices for detecting  $\text{Pb}^{2+}$  in real water samples. The researchers synthesized AgNPs-PVA through a reduction process using  $\text{NaBH}_4$ . After AgNPs and  $\text{Pb}^{2+}$  were immobilized on glass fiber paper, a noticeable color shift occurred, linked to the aggregation caused by the displacement of the stabilizing agent, prompted by the interaction between  $\text{Pb}^{2+}$  ions and PVA molecules. The change in color intensity on the paper was assessed by employing a smartphone and ImageJ software for the quantification of the target analyte.

The synthesis of NPs often involves the chemical reduction process, which employs potentially toxic chemicals like  $\text{NaBH}_4$  and hydrazine. This raises significant environmental and public health concerns. To address this issue, a green synthesis approach<sup>62</sup> can be adopted for NP preparation, utilizing natural sources like plant bark, leaves, and seeds as reducing agents. Previous research has already explored the use of green synthesis to produce AgNPs for portable colorimetric sensing applications. For example, Mavaei *et al.*<sup>63</sup> utilized *Achillea wilhelmsii* (AW) extract to synthesize AgNPs for analysis of  $\text{Hg}^{2+}$  using paper colorimetry. The AgNPs-AW were manually deposited on the paper substrate, and the analyte was added dropwise. The color change from brown to colorless was easily observable by the naked eye. The color transition occurs due to the introduction of  $\text{Hg}^{2+}$  ions into the AgNPs, leading to the formation of amalgam ( $\text{Hg}-\text{Ag}$ ) and subsequent aggregations. The method achieved a low LOD value of 28 nM for detecting  $\text{Hg}^{2+}$ . In another example, Infant and group<sup>64</sup> presented a greener approach for synthesizing AgNPs using *Trigonella*

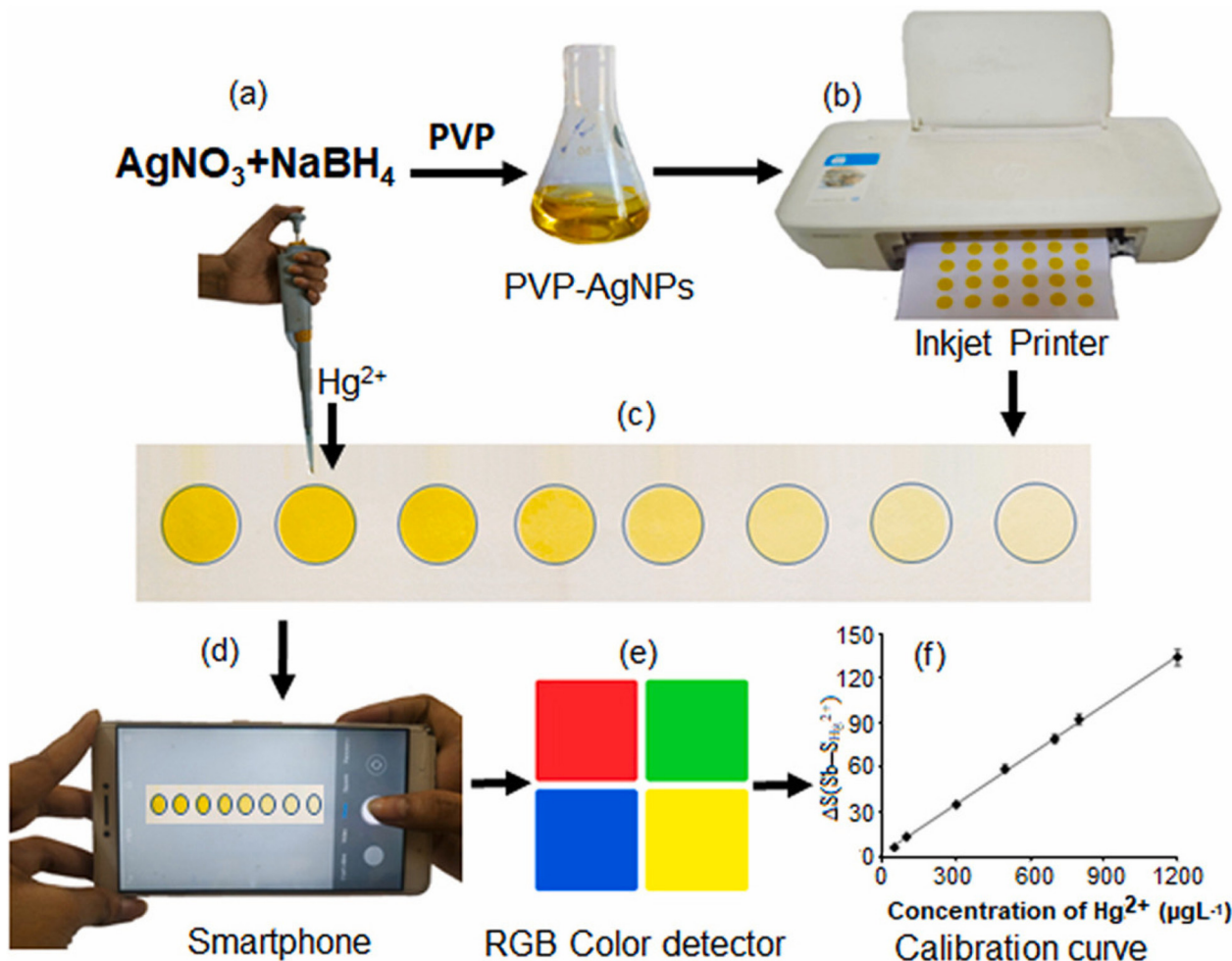


**Fig. 6** Systematic representation of the development of an AgNPs-PVP-based portable colorimetric sensor. (a) Synthesis of AgNPs-PVP. (b) Printing of AgNPs in filter paper. (c) Pipetting  $\text{Hg}^{2+}$  in an AgNP sensing probe. (d) Image captured using a smartphone. (e) RGB value analyzed using ImageJ software. (f) The result as a calibration curve [this figure has been reproduced from ref. 60 with permission from Elsevier Sciences, copyright 2021].

*foenum (Linnaeus)* plant extract, resulting in 27.24 nm cubic-shaped AgNPs. The AgNPs were sprayed onto a paper substrate, and the  $\text{Hg}^{2+}$  analyte was dropwise added to the AgNP-coated paper. The color change was observed without the need for a spectrometer, allowing for simple and direct visual detection. Kahandal and coworkers<sup>65</sup> demonstrated the development of a portable colorimetric sensor for instant paper-based  $\text{Hg}^{2+}$  detection. This sensor utilized green-synthesized AgNPs and was assisted by a smartphone for quick and efficient results. In this article, AgNPs were synthesized from the flower extract of *Acacia nilotica* using a hydrothermal process. Various concentrations of  $\text{Hg}^{2+}$  from 50 to 450  $\mu\text{M}$  were tested. This sensor exhibits excellent selectivity for  $\text{Hg}^{2+}$  as it was successfully tested alongside twelve other heavy metals simultaneously, demonstrating its ability to specifically detect  $\text{Hg}^{2+}$  among a range of potential interfering substances.

**3.2.3 CuNPs.** CuNPs provide several benefits in RGB-based colorimetric sensing application. CuNPs are low cost and show easy aggregation with the target analyte which adds to their accessibility and wide range of applications. However, CuNPs

are highly susceptible to oxidation, which causes a loss in their properties and sensing ability.<sup>66,67</sup> So, synthesis of stabilized CuNPs is a challenging process and some researchers have synthesized stable CuNPs and used as a probe for portable colorimetric sensing application.

For instance, Chandran and colleagues<sup>68</sup> reported the preparation of curcumin functionalized CuNPs (CuNPs-curcumin) for clinically diagnosing  $\text{Na}^+$  ions in both blood serum and urine. CuNPs functionalized with curcumin were produced through a direct chemical reduction process utilizing  $\text{NaBH}_4$  as the reducing agent and curcumin as the stabilizing component. The CuNPs-curcumin were deposited onto cellulose paper strips, and upon immersion in a  $\text{Na}^+$ -containing analyte, a color change from pale yellow to dark yellow occurred. The sensing mechanism was elucidated by examining the interaction between  $\text{Na}^+$  ions and curcumin molecules, leading to the formation of a coordination complex and subsequently causing the aggregation of AuNPs. The RGB color intensity was measured using ImageJ software with a smartphone. Similarly, Ma and Coworkers<sup>69</sup> introduced mercapto-

succinic acid (MSA)-stabilized CuNPs for enzyme-free portable colorimetric sensing of  $\text{H}_2\text{O}_2$  and uric acid (UA) in human urine samples. When UA or  $\text{H}_2\text{O}_2$  molecules came into contact with small CuNPs-MSA, aggregation was induced, resulting in the formation of a violet color. This color change occurred due to the displacement of MSA from the surface of CuNPs. The concentration of UA and  $\text{H}_2\text{O}_2$  was measured by calibrating the change in color intensity using a handheld colorimeter. Furthermore, Ilgar and colleagues<sup>70</sup> demonstrated a green synthesis of CuO NPs through sonication process. Herein, maca extract-coated CuO synthesized for the detection of dopamine is shown in Fig. 7 (a-f). In this article, a smartphone-assisted paper-based colorimetric sensor was developed. The value of LOD calculated was 16.9 nM for dopamine detection using CuO-Maca NPs as a sensing probe.

Karakus *et al.*<sup>71</sup> presented a study involving *Camellia sinensis* polyphenol-capped copper oxide nanoparticles (CuO-PPS NPs) for portable colorimetric sensing of  $\text{NH}_3$ . The researchers utilized a smartphone-based colorimetric method with a paper strip sensor. The CuO-PPS NPs were soaked into the paper sub-

strate and allowed to dry. Upon exposure to  $\text{NH}_3$ , a color change was observed and captured using the smartphone's built-in camera, and the RGB value was calculated using the smartphone for quantitative analysis. Hence, investigating CuNPs for RGB-based colorimetric sensing reveals a cost-effective and versatile solution with easy analyte aggregation. However, CuNPs' susceptibility to oxidation presents a challenge, necessitating stabilization techniques. Successful functionalization of CuNPs for specific applications, like ion diagnosis and molecule detection, highlights their adaptability and potential in colorimetric sensing.

**3.2.4. Bi-metallic NPs (BNPs).** To enhance the sensitivity, selectivity, and response time of portable colorimetric sensing, bimetallic nanoparticles (BNPs) are employed. The combination of two metals not only facilitates on-site analysis and multiplexing, but also enhances stability and response time, making BNPs versatile and efficient for various applications.<sup>72</sup> For instance, Patel and colleagues<sup>73</sup> developed a method for preparing Cu@Ag core-shell NPs for on-site monitoring of dimethoate pesticide in food samples. The introduction of

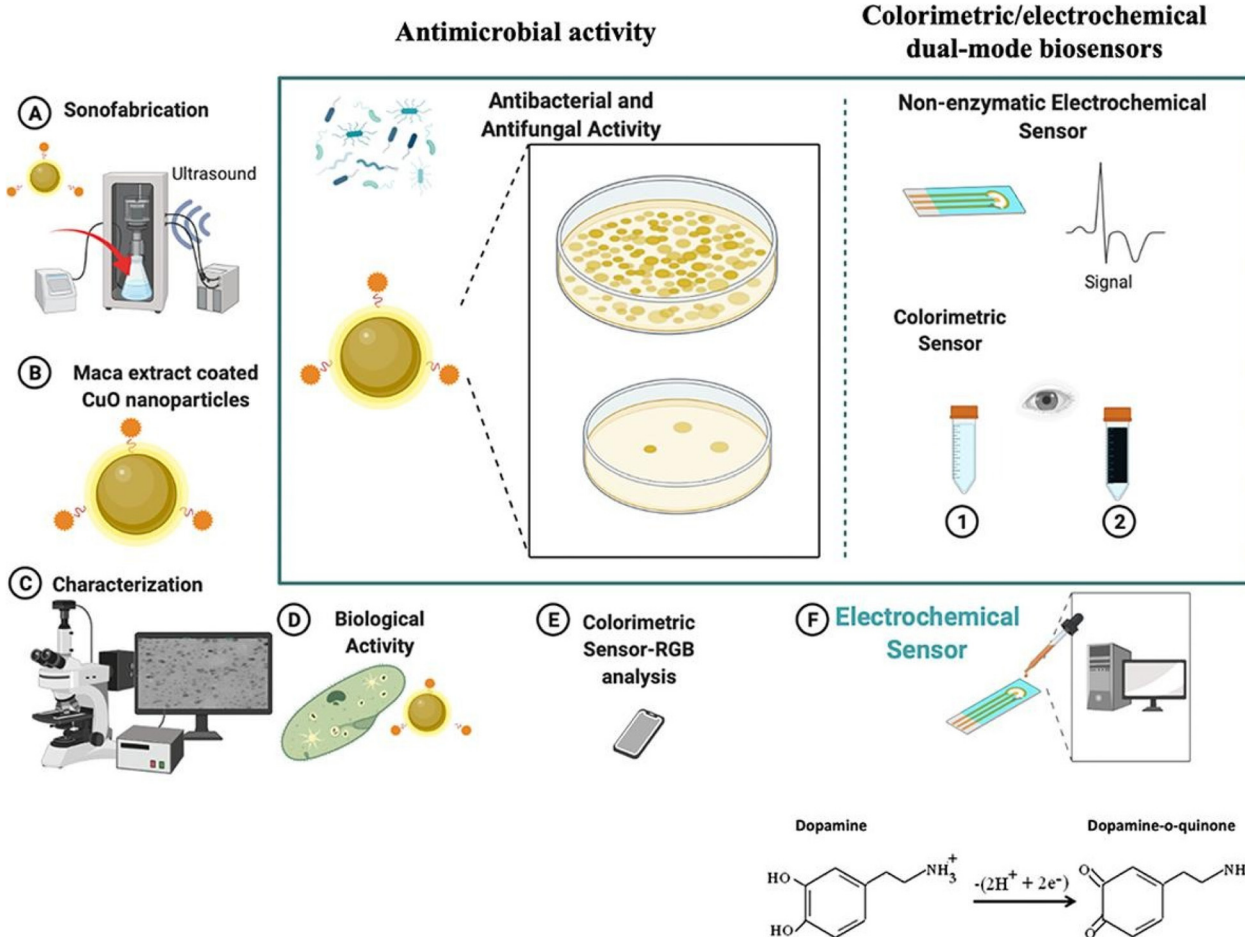


**Fig. 7** CuO-Maca NP-based portable colorimetric/electrochemical sensing of dopamine using the paper-based smartphone sensing technique. (A) Synthesis of CuO-Maca by a sonication method. (B) Image of Maca-CuO NPs. (C) Characterization of CuO-Maca. (D) Antibacterial activity check using CuO-Maca. (E) Smartphone-assisted colorimetric sensing. (F) Portable electrochemical sensing of dopamine [this figure has been reproduced from ref. 70 with permission from Elsevier Sciences, copyright 2022].

dimethoate on printed paper with NPs induced a change in color, attributed to the dimethoate molecule's elevated preference for displacing citrate ions on the NPs' core-shell. Dimethoate molecules primarily interact with Ag in the NPs' core-shell by forming bonds with sulfur or oxygen atoms found in the target pesticide. Different concentrations of pesticides (ranging from 100 to 2000  $\mu\text{g L}^{-1}$ ) were deposited onto the paper, and the change in color intensity was measured using ImageJ software with a smartphone. In another example, Zhang *et al.*<sup>74</sup> synthesized an Au@MnO<sub>2</sub> core-shell nanocomposite for smartphone-assisted monitoring of fish spoilage. A redox process ensued between  $\beta$ -D-glucose pentaacetate and MnO<sub>2</sub>, resulting in a modification of the Au@MnO<sub>2</sub> structure, visibly altering the color of AuNPs from purple to red to the naked eye. RGB analysis was performed using a smartphone for quantitative analysis. The total volatile basic nitrogen level, a common index for measuring fish freshness, was determined using this method.

Moreover, BNPs can be synthesized using both chemical reduction and green synthesis approaches for portable colorimetric sensor applications. For example, Bordbar and colleagues<sup>75</sup> designed bimetallic NPs composed of Au and Ag to detect ignitable liquids in gasoline. They employed a green synthesis approach with lemon juice and orange juice acting as reducing agents, alongside a chemical reduction process exploited the utilization of gallic acid, citrate ions, ascorbic acid, *etc.* When exposed to sample vapors, the sensor underwent aggregation, leading to discernible color alterations in the NPs. These alterations in color were documented with a scanner, ultimately producing unique colorimetric maps for each analyte, facilitating the identification of the tested fuels.

Thus, BNPs enhance portable colorimetric sensing by improving sensitivity, selectivity, and response times. BNPs enable on-site analysis and can be synthesized using eco-friendly methods. Their practical applications, such as pesticide detection and food spoilage monitoring, make them a promising tool for a wide range of applications.

## 4. Recent developments in portable colorimetric sensing devices

### 4.1. Handheld colorimetry devices

Compact, lightweight, and on-site analysis is now possible with portable colorimetric sensing devices, thanks to recent advancements in miniaturization and integration, which eliminate the need for elaborate laboratory setups. In this way the work of miniaturization and integration is happening very fast in the development of portable chemical sensing device. For example, Mukherjee *et al.*<sup>38</sup> designed a handheld, cheap, and portable colorimetric device for the rapid estimation of sub ppm level of F<sup>-</sup> ion in water. This device was prepared *via* the combination of LEDs and a photodiode with smartphone attachment. This innovative sensing approach utilizes core-shell NPs (ceria@zirconia nanocages) in combination with a chemo-responsive dye (xylenol orange) to detect fluoride ions

(F<sup>-</sup>). The developed sensor exhibits remarkable selectivity for F<sup>-</sup> and demonstrates exceptional sensitivity within the 0.1–5 mg L<sup>-1</sup> range in water samples. Upon interaction with F<sup>-</sup>, these NPs undergo a rapid color transition from red to yellow, even at sub-ppm levels. Extensive testing involved the detection of F<sup>-</sup> ions from water samples from different regions, mouthwash, dental care products, and toothpaste, employing both a smartphone attachment and visual detection for device validation. The device performed better than the earlier methods for aqueous F<sup>-</sup> sensing. Laganovska and coworkers<sup>37</sup> designed a handheld spectrophotometer for solution-based colorimetric application. Herein, the completed instrument has a resolution of 15 nm and can measure absorption in the 450–750 nm wavelength region. Tests in three separate areas to identify the LOQ, LOD, and RSD% was performed after the device's assurance, which involved evaluating the system's wavelength precision, range of detection, and the proportion of signal to noise. According to the results, this fabricated device showed similar function to highly priced spectrophotometers. The design and electrical parts of a portable handheld colorimetry device are shown in Fig. 8.

Srivastava and coworkers<sup>76</sup> developed a portable spectrometer designed for the measurement of Fe<sup>3+</sup> and Cu<sup>2+</sup> in drinking water samples. The spectrometer consists of a radiation source using a white LED and a spectral sensor (AS7262) designed for the detection of visible radiation. An energy-efficient wireless embedded platform operating at sub-GHz frequencies was engineered and connected to both the light source and detector. The accuracy and precision of the device was tested using the commercially available HANNA colorimetric instrument. Inamori and colleagues<sup>77</sup> developed a wearable colorimetric device for real-time monitoring of jaundice and vital signs. The incorporation of four LEDs in the device measures the SpO<sub>2</sub> levels, bilirubin and heart rate in neonates. The fabrication of a polydimethylsiloxane (PDMS) lens in the device amplifies the signals reflected from LEDs. A smartphone and a personal computer can be used as processing and display systems. Kumar and coworkers<sup>78</sup> reported the use of a handheld device for As<sup>3+</sup> analysis in water samples. In their approach, As<sup>3+</sup> was mixed with KIO<sub>3</sub> to undergo an oxidation reaction, converting As<sup>3+</sup> to As<sup>5+</sup> and liberating iodine. This reaction caused the color to change from red to colorless. A calibration plot was drawn to determine the unknown concentration of As<sup>3+</sup> based on the observed color change. Yu and team<sup>79</sup> developed a cost-effective, wireless, and handheld spectrophotometer designed for the colorimetric analysis of DNA, BSA, and Cu<sup>2+</sup> metal ions. They assembled various components using 3D printing technology. The device can scan samples within the 405–690 nm wavelength range, and an Android application, connected *via* bluetooth, was employed for measuring the absorbance of solutions. The device demonstrated sensitivity on par with that of a commercial spectrophotometer. This device finds practical utility in analyzing fluid samples across a range of fields, environmental, biological and clinical diagnostics.



Fig. 8 Portable handheld colorimetric detection of phosphate [this figure has been reproduced from ref. 37 under open access article in terms of the Creative Commons CC-BY license].

These studies are of significant importance as they introduce compact and cost-effective technologies for chemical analysis, enabling on-site assessments without the need for extensive laboratory setups. This accessibility to rapid and accurate chemical sensing has broad implications, ranging from ensuring safe drinking water quality to monitoring vital signs in healthcare, ultimately enhancing our ability to address environmental, biological, and clinical challenges efficiently and affordably.

#### 4.2. RGB-based colorimetry

Approaches for portable solution-based colorimetric sensors have many advantages. Rapid and on-the-spot analyses of diverse array substances, such as pollutants, infections, or chemicals, are made possible by these small, user-friendly instruments. They give results instantly, eliminating the requirement for any rigid or flexible substrate for the implantation of the sensing probe. A smartphone or handheld color detectors were used to measure the solution's color change. They are useful for environmental monitoring, medical diagnostics, and guaranteeing safety in numerous industries for their adaptability and simplicity of use. For example, Shahvar and coworkers<sup>40</sup> designed a solution-based portable colorimetric device to detect water containing an ethanolic solution.  $\text{CoCl}_2$  was used as a sensing probe, and the sensing mechanism relied on the formation of a  $[\text{Co}(\text{EtOH})_2\text{Cl}_2]$  complex, which resulted in a blue color when added to water. However, when ethanolic solution was introduced, the blue color faded, and a pink color appeared due to the formation of  $[\text{Co}(\text{H}_2\text{O})_6]^{2+}$ . The device comprised of a cubic box made from blue plexiglass sheets, with a 2 mL polypropylene transparent Eppendorf tube used as the sample holder. RGB value analysis

was conducted using an Android application called 'Rang-Snehas'. Another study, the colorimetric sensing strategy presented in this article, allows for the estimation of bovine serum albumin (BSA), enzymes, and carbohydrates macromolecules using Lowry's assay and Anthrone's assay. To facilitate the process, a cubic designed nylon sheet was attached to a smartphone. In this arrangement, a 3 V battery-powered white LED bulb was incorporated, and the emitted light was focused by a plano-convex lens. A 5 mm quartz cuvette could be inserted into the setup, allowing light to pass through it. Next, the sample solution was introduced into the cuvette, and the setup was illuminated through a nylon diffuser. Utilizing a smartphone, images of the illuminated cuvette were taken and subsequently used for the analysis. This analysis aimed to estimate the concentration of the target macromolecules by assessing the color changes as observed in the course of Lowry's and Anthrone's assays.<sup>41</sup> The fabrication process of a solution-based colorimetric sensor is shown in Fig. 9.

Safranko and team<sup>80</sup> developed an image processing software for quantification of chemical substances through digital colorimetric imaging. Here, digital imaging devices such as smartphones and cameras are exploited for taking the images of  $\text{CuSO}_4$  (blue),  $\text{CoSO}_4$  (red),  $\text{KMnO}_4$  (purple), and  $\text{NiSO}_4$  (green) solutions of different concentrations. The image processing software ColorX was used to calculate the concentration of unknown colored solution using RGB values through measurements. This approach holds significant educational value for students, serving as a valuable tool and a learning model. In a study led by Rajamanikandan *et al.*,<sup>81</sup> they illustrated a colorimetric detection technique for  $\text{Cr}^{3+}$  in environmental water using smartphones. The analysis relied on utilizing the RGB color ratio for  $\text{Cr}^{3+}$  analysis in the water

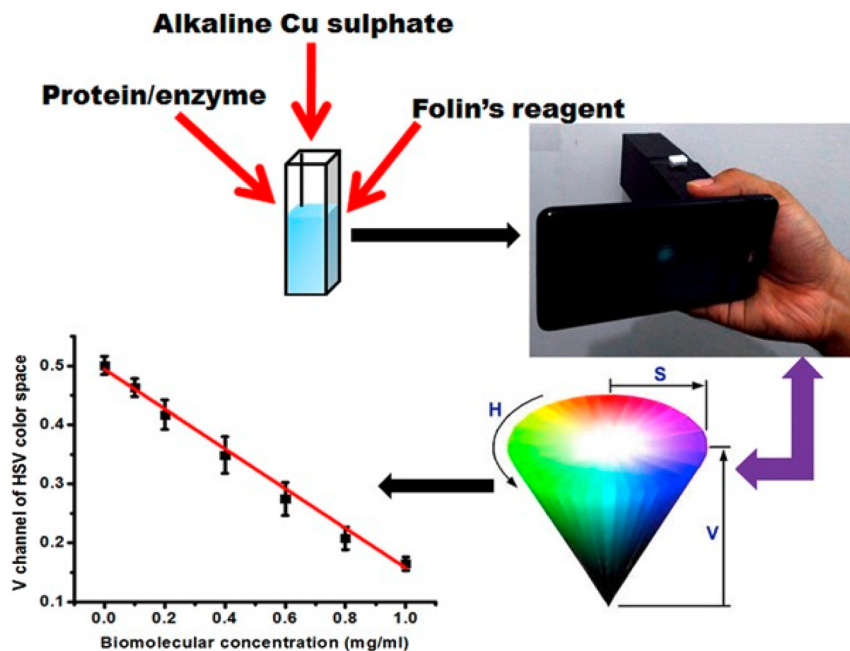


**Fig. 9** Solution-based portable RGB analysis using a smartphone [this figure has been reproduced from ref. 41 with permission from Wiley Sciences, copyright 2017].

samples. In this process, the introduction of  $\text{Cr}^{3+}$  into mercapto-5-methyl-1,3,4-thiadiazole (MMT)-modified AuNPs resulted in the release of MMT from the NP surface, forming a distinctive colored complex with the target analyte, which was subsequently measured using a smartphone.

RGB-based colorimetry is pivotal for its ability to provide quick and on-the-spot detection of a wide range of substances, from contaminants to analytes, using portable and user-friendly devices. This technology offers rapid results without the need for complex laboratory setups, making it highly adaptable for applications in environmental monitoring, medical diagnostics, and industrial safety.

#### 4.3. Paper-based RGB/grey scale colorimetry

Paper-based RGB/grey scale colorimetry is a method that employs paper as a substrate for colorimetric measurements using a smartphone as the sensing device. The development of smartphones has completely changed how portable colorimetric sensors are made. By capturing images of samples or color patches on the paper and analyzing their RGB or grey scale values, this technique enables rapid and cost-effective quantification of analytes and color changes. It finds applications in diverse fields, from chemical analysis to environmental monitoring, offering a simple and portable solution for color-based assessments. Real-time analysis, data storage, and remote monitoring are made possible by smartphone integration, creating new opportunities for quick and convenient colorimetric sensing applications.

Shrivastava and co-workers<sup>82</sup> engineered a portable colorimetric detector that operates with smartphones to sense  $\text{As}^{3+}$  in water and soil samples. Their method involved employing sucrose-

capped AuNPs as a nanoprobe and depositing 50  $\mu\text{L}$  of these NPs onto wax treated filter paper. Following this, different concentrations of  $\text{As}^{3+}$  were introduced for analysis, and the alterations in color intensity were quantified using ImageJ software. A calibration curve was then constructed to interpret the results. Dong *et al.*<sup>83</sup> presented a novel smartphone-based sensing approach for detecting  $\text{PO}_4^{3-}$  in food samples, based on color changes resulting from the aggregation and anti-aggregation of PVP-modified AgNPs induced by  $\text{Pb}^{2+}$  and  $\text{PO}_4^{3-}$ , and measurements were made using the 'Color-Assist' app on a smartphone. Wang and coworkers<sup>84</sup> introduced a smartphone-based plasmonic sensing system coupled with image processing, illustrating two colorimetric biochemical sensing concepts based on nano plasmonic phenomena, significantly improving the LOD, and demonstrating its potential for point-of-care and early kidney disease detection in urine testing. Dong and group<sup>85</sup> proposed a smartphone-based colorimetric detection approach for thiosulfate ( $\text{S}_2\text{O}_3^{2-}$ ), utilizing tannic acid-stabilized AgNPs mixed with different concentrations of  $\text{S}_2\text{O}_3^{2-}$ , and recording color intensity changes using the 'Color-Assist' app, effectively estimating unknown concentrations of  $\text{S}_2\text{O}_3^{2-}$  in agricultural samples. Li and group<sup>86</sup> demonstrated a smartphone-based colorimetric sensing approach for detecting ascorbic acid (AA) in tropical fruits. Here a material called Fe-single atom non-enzyme (Fe-SAN), synthesized from green tea leaves and  $\text{NaH}_2\text{PO}_4$ , resulted in a change in the color of 3,3',5,5'-tetramethylbenzidine from colorless to blue. The introduction of AA effectively prevented this color transformation of the dye. This mechanism offered a better LOD, facilitating the estimation of AA concentrations in a variety of fruits. Choudhary *et al.*<sup>87</sup> demonstrated a paper-

based colorimetric sensor utilizing brilliant green (BG) as a probe for detecting phosphate ions in drinking water. A Whatman filter paper strip was prepared using a dip coating method, ultrasonicated with the 'Tween-80' surfactant, and soaked with an acidified ammonium molybdate solution. BG solution was then deposited on the paper strip. In the absence of phosphate ions, the probe appeared as a pale-yellow color. Subsequently, different concentrations of phosphate ions from 13.6 to 0.27 mg L<sup>-1</sup> were added at various pH levels, and the color change was measured using ImageJ software. The LOD value was calculated 0.07 mg L<sup>-1</sup>. High concentrations led to a color change to green, while low concentrations resulted in a loss of color intensity and a shift to yellow, as illustrated in Fig. 10.

Firdaus and colleagues<sup>88</sup> developed a paper-based sensor using stabilized AgNPs for rapid analysis of Hg<sup>2+</sup> ions. A hydrophobic ink and nanomaterials (NMs) were printed on paper substrates, resulting in a color change from pale yellow to colorless when mercury ions were added. The RGB intensity change was measured using 'MATLAB' software, and a calibration curve was plotted to determine unknown concentrations of analytes. Zhu and group<sup>89</sup> demonstrated a paper-colorimetric strip coated with polysulfobetaine methacrylate (pSBMA) for the determination of three pesticides (cypermethrin, profenofos, and chlorpyrifos).

The paper sensor was developed by depositing the zwitterionic polymer pSBMA on a glass substrate using PDMS, with cellulose filter paper as the selected material. When pesticides were added to this paper sensor, a color change was observed, and the color intensity was optimized using 'ImageJ' software, resulting in LOD values of 0.235 mg L<sup>-1</sup> for chlorpyrifos, 4.891 mg L<sup>-1</sup> for profenofos, and 4.053 mg L<sup>-1</sup> for cypermethrin. Kong *et al.*<sup>90</sup> designed a paper sensor based on ZnFe<sub>2</sub>O<sub>4</sub> magnetic NPs (ZnFe<sub>2</sub>O<sub>4</sub> MNPs) for colorimetric detection of bisphenol A. The sensor's adsorption capacity was evaluated using an adsorption isotherm model, where ZnFe<sub>2</sub>O<sub>4</sub> MNPs and paper were wrapped with a molecular imprinted polymer (MIP). The sensor exhibited a gray intensity that corresponded to the concentrations of bisphenol-A, possessing a LOD of 6.18 nM, making it suitable for environmental monitoring, security inspection, and complex matrices. Ratnarathorn and colleagues<sup>91</sup> demonstrated a paper-based analytical device (PAD) designed for the colorimetric detection of Cu<sup>2+</sup> in water samples. The sensing probe, consisting of thiol-modified AgNPs on a paper substrate, displayed a transition in color, shifting from pale yellow to shades of orange and green-brown upon the introduction of Cu<sup>2+</sup>. The color intensity change was measured using 'Adobe Photoshop CS2' software, and a calibration curve was plotted,

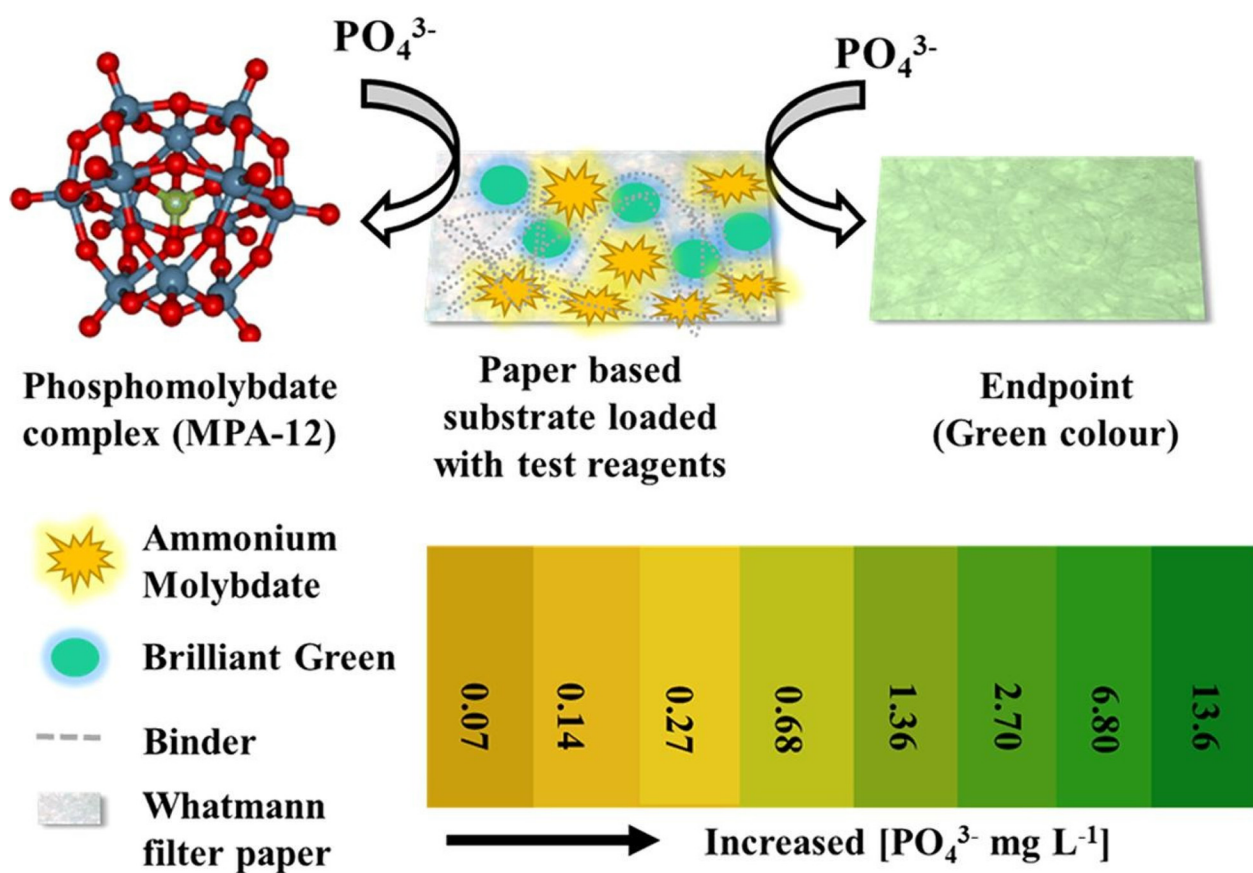


Fig. 10 A paper-based colorimetric sensor formulated with ammonium molybdate and BG for the detection of phosphate ion in drinking water [this figure has been reproduced from ref. 87 with permission from Elsevier Sciences, copyright 2021].

resulting in a LOD value of  $0.5 \mu\text{g L}^{-1}$  observed by the naked eye. Silva and colleagues<sup>92</sup> introduced a new sensing strategy utilizing a paper substrate for the identification of phenacetin in cocaine samples. The proposed approach utilizes white office paper with detecting zones created using wax printing technology. A chromophoric material (1,2-naphthoquinone-4-sulfonate) was spotted on the paper, and upon adding an alkaline cocaine sample, resulting in a distinct color transition from colorless to violet. The color alteration was quantified using 'GIMP2' software, and a calibration curve was generated for varying concentrations of cocaine, yielding a LOD of  $3.5 \mu\text{g L}^{-1}$ . Zhang *et al.*<sup>93</sup> demonstrated a paper-based sensor for the recognition of biomarkers related to  $\text{H}_2\text{O}_2$ , using glucose oxidase as an example. In the presence of  $\text{H}_2\text{O}_2$ , KI can catalyze the oxidation of tetramethylbenzidine to colorize the paper-based sensing region. The color intensity was photographed using a scanner and the change in the intensity of RGB value was analyzed using Adobe Photoshop, making it an affordable, ecologically safe, and simple technique for testing  $\text{H}_2\text{O}_2$ -related biomarkers at the point of care. Paper-based colorimetric devices are well-suited for point-of-care applications in resource-constrained environments due to their user-friendliness, affordability, and disposability.<sup>94</sup> These advancements drive innovation in portable colorimetric sensing, expanding its potential applications in healthcare, environmental monitoring, food safety, and other domains.

Paper-based RGB/grey scale colorimetry, when combined with smartphones or portable sensing devices, offers a transformative approach to portable and cost-effective colorimetric sensing for measuring diverse chemical substances. Its user-friendly and disposable nature, along with real-time data capture, makes it a valuable tool for addressing critical challenges in healthcare, environmental protection, and food quality assurance. These studies demonstrate its practical applications in fields like environmental monitoring, healthcare, and food safety, particularly in resource-limited settings.

#### 4.4. Wearable colorimetry

The latest advancement in portable colorimetric sensors is the wearable colorimetric sensor, which offers regular health monitoring for patients with several advantages. This type of sensor is flexible and stretchable, easily attachable to the body using cloth or synthetic tape, allowing patients to carry out their daily routines comfortably while being monitored. Wearable colorimetric sensors are particularly useful for patients who require daily health monitoring, such as those with diabetes or hypertension. Researchers are increasingly focusing on developing such sensors. For instance, Xiao and team<sup>95</sup> demonstrated a wearable colorimetric sensor for monitoring glucose levels released in sweat. This microfluidic chip-based sensor is designed to detect glucose in sweat and features five microfluidic channels connected to detection micro-chambers with integrated check valves to prevent backflow. The microchambers contain glucose oxidase-peroxidase-*o*-dianisidine reagents, providing a more sensitive response to glucose compared to conventional systems. The sensor enables

simultaneous detection in five channels, with a linear range of 0.1–0.5 mM and a LOD of 0.03 mM. Tests on sweat samples from fasting and postprandial subjects demonstrated the sensor's ability to detect subtle differences in sweat glucose concentration. Another example is the work of Finnegan *et al.*<sup>96</sup> who designed a colorimetric wearable skin surface pH sensor using a bromocresol green sol-gel (BCG-sol-gel) dye-spotted cellulose substrate. The sensor spots undergo a color change upon the release of basic volatile nitrogen molecules, such as ammonia and amines, from the skin. The sensor utilizes 6 spots of BCG deposited on a cellulose substrate and affixed to the palms of both male and female subjects using a PET substrate. The colorimetric sensor is designed with a 3-layer material, comprising a first layer of a stainless-steel woven wire mesh and a second layer of a cellulose substrate with the 6 BCG sensors. The final layer is a cover layer made from the PET film and the complete platform was enclosed as shown in Fig. 11 (a–c). Color changes were measured before and after use by ImageJ software, a calibration curve was plotted and the skin surface pH value using this wearable sensor was measured.

Hwang and colleagues<sup>97</sup> introduced a flexible wearable  $\text{H}_2$  gas sensor based on  $\text{PdO}@\text{ZnO}$  with a polyacrylonitrile composite, formed through an electrospinning process on polyacrylamide and coated with polydimethylsiloxane, showing a color change due to the conversion of  $\text{PdO}$  into  $\text{Pd}$  NPs upon  $\text{H}_2$  gas adsorption, with the color intensity measured using a detector and a LOD value of 1000 ppm for  $\text{H}_2$  gas. Ha *et al.*<sup>98</sup> presented a wearable sweat pH sensor fabricated using curcumin and thermoplastic polyurethane for pH measurement *via* a color change reaction from enol to di-keto form. This sensor can be seamlessly affixed to a range of fabric materials through  $\text{O}_2$  plasma activation and thermal heating, making it a promising tool for continuous sweat pH monitoring, particularly beneficial for individuals with cystic fibrosis.

You and colleagues<sup>99</sup> designed wearable multi-groove micro-needles for colorimetric monitoring of glucose levels in diabetic patients, employing microneedles prepared by photopolymerization of polyethylene glycol di-acrylate to penetrate the patient's skin, and extract internal fluid *via* a capillary process, with successful application demonstrated on mice for glucose monitoring. Zhang *et al.*<sup>100</sup> demonstrated a flexible and stretchable colorimetric sensor for monitoring pH and ion concentrations. It features super hydrophilic assays made from thermoplastic polymer nanofiber textiles and silica NPs, combined with a superhydrophobic material for sweat focusing, with color changes efficiently measured using a smartphone.

Recent developments in portable colorimetric sensor technologies have brought positive impacts on sensing applications. Miniaturization and integration enable the development of small lightweight sensors that offer convenience for on-site and real-time analysis, eliminating the need for complex laboratory preparations.<sup>42,101</sup> Wearable colorimetric sensors enable continuous monitoring and personalized healthcare, facilitating real-time identification of environmental and medical issues.<sup>102</sup> He and his research group<sup>103</sup>

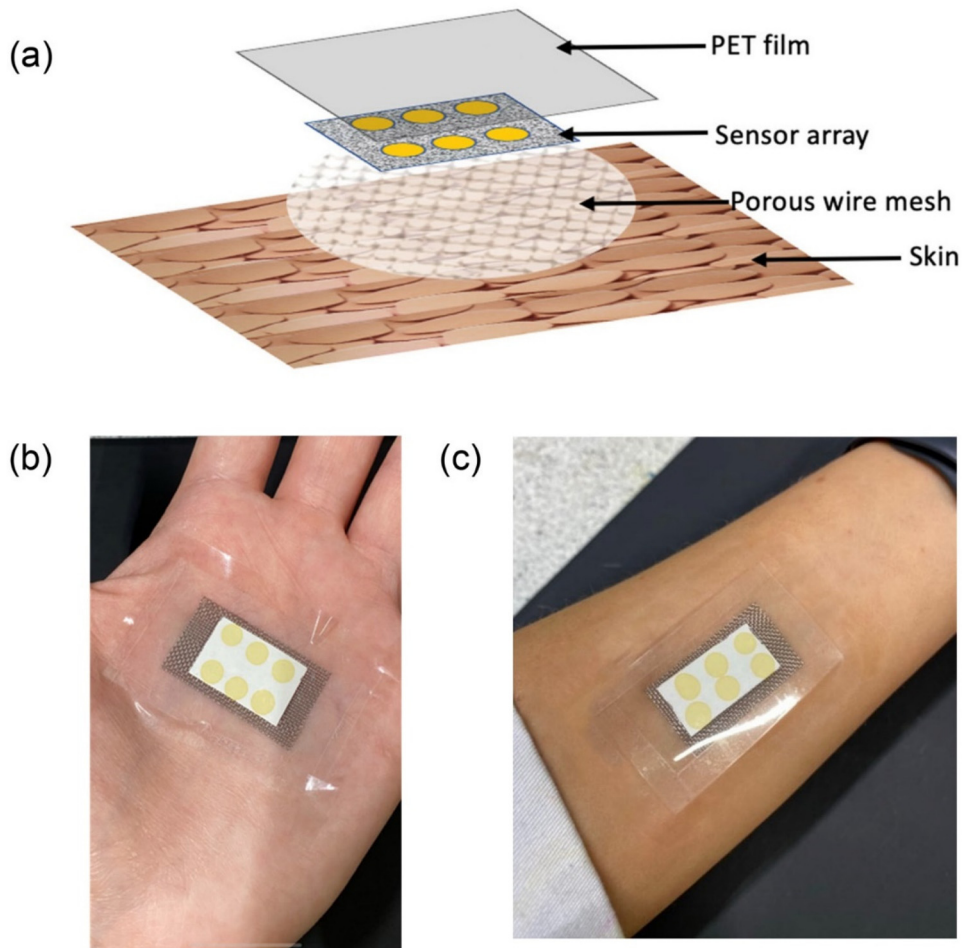


**Fig. 11** A BCG sol–gel dye-spotted cellulose substrate-based colorimetric wearable skin surface pH sensor. (a) Three layers of the sensor, (b) the sensor tapped on a palm and (c) the sensor tapped on the wrist [this figure has been reproduced from ref. 96 under open access article in terms of the Creative Commons CC-BY license].

developed adaptable, skin-mounted colorimetric bands to monitor chloride, pH, calcium, and glucose levels in sweat samples. These bands use a superhydrophobic silica coating to channel sweat away from the skin into superhydrophilic micropatterns. The colorimetric changes are captured using a smartphone camera, allowing for precise quantitative analysis. This method offers a straightforward and user-friendly approach for health diagnostics in clinical settings. However, it is worth noting that these bands do not provide real-time monitoring and are affected by variations in the sweat rate. Xu *et al.*<sup>104</sup> presented a novel technology, super-wettable microchips, for the colorimetric monitoring of glucose, calcium, and protein levels in the microgravity environment of the human body to track daily physiological variations. The team developed a superhydrophobic substrate and super-hydrophilic microwells, which serve as channels for collecting tiny sweat droplets. These collected samples were then subjected to specific reagents within the microchips, resulting in observable color changes. These color changes were documented using a camera to establish grayscale values for precise quanti-

tative analysis. This compact device is user-friendly, lightweight, and doesn't require any electrical equipment for operation. Wu and colleagues<sup>105</sup> carried out nucleic acid detection using a super-hydrophilic cotton thread. They initially loaded GNP/DNA conjugates onto a designated pad. Following the deposition of a sample containing the target DNA, a red-colored absorption band became visible to the naked eye after 15 min incubation. Quantitative analysis was performed by recording the optical density of the color band using a specialized instrument referred to as the “strip reader”, in combination with software provided by “GoldBio”.

Wearable colorimetry is a game changer in healthcare and environmental monitoring, allowing real-time tracking of parameters like glucose levels in sweat and skin surface pH changes. These sensors offer personalized and continuous health monitoring, enabling quick detection of medical issues and environmental factors. They also hold the potential for enhancing safety by monitoring gas concentrations in real time, promising a transformative impact on health and environmental monitoring.

## 5. Applications of portable colorimetric sensing devices

### 5.1 Environmental monitoring

Portable colorimetric sensing plays a crucial role in environmental monitoring, enabling quick and effective analysis of pollutants and toxins in air, water, and soil. Utilizing nanomaterials and user-friendly tools, on-site testing becomes more accessible, allowing environmental establishments and researchers to monitor pollution levels promptly, contributing to a healthier planet. Sargazi and Kaykhai<sup>106</sup> developed a cost-effective portable smartphone-based spectrophotometer for measuring trace levels of  $\text{Cl}^-$  and  $\text{NO}_2^-$  in water samples. The device, made of plexiglass with LEDs and a piece of DVD acting as a light dispersing element, used the smartphone's battery for power and spectrum analysis. The spectrophotometer produced a LOD of  $0.05 \text{ mg L}^{-1}$  for  $\text{Cl}^-$  and  $0.008 \text{ mg L}^{-1}$  for  $\text{NO}_2^-$ , while exhibiting linear ranges from 1.00 to  $4.00 \text{ mg L}^{-1}$  for  $\text{Cl}^-$  and 0.05 to  $1.20 \text{ mg L}^{-1}$  for  $\text{NO}_2^-$ . These results are in close agreement with established standard methods. Li and group<sup>107</sup> presented a flexible and robust algorithmic model for simulating and analyzing the transformation of spectral data acquired using a camera into RGB values. The proposed algorithm showed good linearity and precision, making it suitable for quantifying various nutrients in natural water. Field measurements of five different nutrients using the algorithm produced results consistent with conventional methods. Cao *et al.*<sup>108</sup> described a colorimetric detection procedure for  $\text{Cu}^{2+}$  using the pigment obtained from red beet as a colorimetric probe. The pigment exhibited a selective response to  $\text{Cu}^{2+}$  in an alkaline environment, leading to a distinct shift in color from purple to orange-red. An android-based app was developed to detect  $\text{Cu}^{2+}$  visually by identifying the RGB value of the colorimetric probe solution, successfully verifying  $\text{Cu}^{2+}$  detection in drinking water. Liu and co-workers<sup>109</sup> reported a simplified portable method for the measurement of  $\text{Fe}^{3+}$  using rhodamine-grafted paper as a sensing material. A smartphone was employed for recording the signal intensity. The method achieved a detection limit of  $1.4 \text{ }\mu\text{M}$  for analysis of  $\text{Fe}^{3+}$  in water samples.

Srivastava and Sharma<sup>76</sup> developed a smartphone application-based portable spectrophotometer to stabilize and enable on-site monitoring of  $\text{Fe}^{3+}$  and  $\text{Cu}^{2+}$  ions in drinking water. The system's optimization included the use of standard buffer samples with known concentrations of  $\text{Fe}^{3+}$  and  $\text{Cu}^{2+}$  prior to the analysis of water samples, covering a concentration range of 0.001–5 ppm for heavy metals. Rajamanikandan *et al.*<sup>81</sup> introduced a novel method to detect  $\text{Cr}^{3+}$  ions using a smartphone. The method covers a broad linear range (40–128 nM) and possesses a low LOD of 12.4 nM. Esfahani and group<sup>57</sup> employed an AuNPs-MMA for portable colorimetric detection of phosphate ions in drinking water. By introducing  $\text{Eu}^{3+}$  ions, the AuNPs aggregate, changing their color from blue to red, enabling sensitive and selective phosphate detection with a low LOD of  $0.3 \text{ }\mu\text{g L}^{-1}$ . Notably, the method demon-

strated a commendable LOD value, estimated at  $0.3 \text{ }\mu\text{g L}^{-1}$ . Budlayan and coworkers<sup>110</sup> demonstrated a paper-based colorimetric sensor based on thiamine-functionalized AgNPs for the on-site detection of  $\text{Hg}^{2+}$ . Herein, the sensor can detect  $\text{Hg}^{2+}$  with a noticeable detection range of up to 0.5 M when the color changes from yellowish to white. For samples of tap water and creek water spiked with  $\text{Hg}^{2+}$ , the sensor's colorimetric response is constant and selective towards  $\text{Hg}^{2+}$ . Rajamanikandan *et al.*<sup>111</sup> demonstrated cysteine-functionalized AgNPs (Cys-AgNPs) for the smartphone-coupled paper-based colorimetric method for the analysis of toxic sulfide ions ( $\text{S}^{2-}$ ). Herein, in 2 min following the addition of  $\text{S}^{2-}$  ions, the colour of Cys-AgNPs changed from yellow to colorless. The large linear range from 40 to  $480 \text{ }\mu\text{M}$  for determination of  $\text{S}^{2-}$  ion was obtained with LOD value of 28 nM. In addition, various NMs such as Ag, Au, and Cu NPs and chromophoric dyes<sup>112–120</sup> have been frequently used for the determination and on-site detection of environmental toxic metals and pollutants. Table 1 provides an overview of the environmental uses of portable colorimetric sensors for analyzing various chemical species in water samples.

Hence, the development of portable smartphone-based spectrophotometers and the colorimetric detection method has greatly advanced environmental monitoring. These cost-effective innovations enable on-site quantification of trace levels of various substances, including chlorine, nitrite,  $\text{Cu}^{2+}$ ,  $\text{Fe}^{3+}$ , and  $\text{Cr}^{3+}$ . By using readily available materials and smartphone applications, they provide efficient, rapid, and reliable results comparable to traditional laboratory methods. These technologies hold promise for environmental scientists and field personnel in safeguarding public health and the environment, making them valuable tools for water analysis and environmental monitoring.

### 5.2 Clinical and point-of-care diagnostics

Portable colorimetric sensing has revolutionized point-of-care diagnosis, enabling rapid and reliable analyses at the patient's bedside or in remote areas, benefiting healthcare personnel and patients with better outcomes and disease management. Integration of nanomaterials and smartphone-based systems allows on-the-spot analyses of various analytes, including infections, biomarkers, and biomolecules. Srivastava *et al.*<sup>121</sup> developed a paper-based colorimetric sensor for glucose monitoring based on a novel nanzyme ( $\text{CuO}@\text{rGO}$ ), formed by coating rGO sheets with CuO NPs by an ultrasonication process. Herein, the sensor has a lower detection limit of between 7.0 and 8.0 M and strong selectivity. The sensor has the potential to provide a simple, affordable, portable, smartphone-assisted digital image colorimetry for the sensitive and selective measurement of glucose in human blood samples. Santos and colleagues<sup>122</sup> illustrated a smartphone-based colorimetric portable sensor based on AuNPs-PVA decorated with methyl orange (MO) azo dye (AuNP@PVA@MO) for the determination of  $\text{H}_2\text{O}_2$ . Herein, chemometric modelling makes it possible to visually detect  $\text{H}_2\text{O}_2$  with a detection limit of 1.70 mM, encouraging the use of nanomaterial sensors and

**Table 1** Overview of the environmental uses of portable colorimetric sensors for analyzing various chemical species in water samples

| Materials/probe                       | Substrate             | Sensing method         | Analyte                     | Linearity range              | LOD                        | Samples          | Ref. |
|---------------------------------------|-----------------------|------------------------|-----------------------------|------------------------------|----------------------------|------------------|------|
| Fuchsin dyes                          | Filter paper          | Smartphone/RGB         | $\text{NO}_2^-$             | 0.005–9.2 mg L <sup>-1</sup> | —                          | Water            | 49   |
| AuNPs-GSH                             | PET paper             | Visual detection       | $\text{Cd}^{2+}$            | 10–100 nM                    | 18.8 nM                    | Potable water    | 53   |
| AuNPs-VPA                             | Filter paper          | Smartphone/RGB         | $\text{UO}_2^{2+}$          | —                            | 2.0 $\mu\text{M}$          | Water            | 54   |
| AuNPs-aptamer                         | Solution              | Smartphone/RGB         | $\text{Cd}^{2+}$            | 2–20 $\mu\text{g L}^{-1}$    | 1.12 $\mu\text{g L}^{-1}$  | Water            | 56   |
| AuNPs-MACA                            | Solution              | Visual detection/LSPR  | $\text{PO}_4^{2-}$          | 0.3 $\mu\text{g L}^{-1}$     | 10–26 $\mu\text{g L}^{-1}$ | water            | 57   |
| AgNPs                                 | Filter paper          | Smartphone/RGB         | $\text{Hg}^{2+}$            | 40–1200 $\mu\text{g L}^{-1}$ | 10 $\mu\text{g L}^{-1}$    | Water            | 60   |
| AgNPs-PVA                             | Filter paper          | Smartphone/RGB         | $\text{Pb}^{2+}$            | 50–1000 $\mu\text{g L}^{-1}$ | 20 $\mu\text{g L}^{-1}$    | Water            | 61   |
| AgNPs-AW                              | Filter paper          | Smartphone/RGB         | $\text{Hg}^{2+}$            | 100 nM–100 $\mu\text{M}$     | 28 nM                      | Water            | 63   |
| AgNPs- <i>Acacia nilotica</i>         | Filter paper/solution | Smartphone/RGB         | $\text{Hg}^{2+}$            | 50–450 $\mu\text{M}$         | —                          | Water            | 65   |
| AuNPs-MMT                             | Filter paper          | Smartphone/RGB         | $\text{Cr}^{3+}$            | 40–128 nM                    | 12.4 nM                    | Water            | 81   |
| AuNPs/sucrose                         | Filter paper          | Smartphone/RGB         | $\text{As}^{3+}$            | 50–3000 $\mu\text{g L}^{-1}$ | 20 $\mu\text{g L}^{-1}$    | Water and soil   | 82   |
| AgNPs-PVP                             | Filter paper          | Smartphone/RGB         | $\text{P}_2\text{O}_7^{4-}$ | 0.2–2 $\mu\text{M}$          | 0.2 $\mu\text{M}$          | Water            | 83   |
| AgNPs                                 | Filter paper          | Smartphone/RGB         | $\text{S}_2\text{O}_3^{2-}$ | 0–20 $\mu\text{M}$           | 1.0 $\mu\text{M}$          | Water            | 85   |
| BG-triaryl methane dye                | Filter paper          | Visual detection       | $\text{PO}_4^{2-}$          | 13.6–0.27 mg L <sup>-1</sup> | 0.07 mg L <sup>-1</sup>    | Water            | 87   |
| AgNPs                                 | Filter paper          | Smartphone/RGB         | $\text{Hg}^{2+}$            | —                            | 0.86 $\mu\text{g L}^{-1}$  | River water      | 88   |
| ZnFe <sub>2</sub> O <sub>4</sub> MNPs | Cellulose paper       | Visual detection       | Bisphenol-A                 | 10–1000 nM                   | 6.18 nM                    | Water            | 90   |
| AgNPs                                 | Filter paper          | Visual detection       | $\text{Cu}^{2+}$            | 7.8–62.8 $\mu\text{M}$       | 7.8 nM                     | Water            | 91   |
| AgNPs-thiamine                        | Filter paper          | Portable/RGB           | $\text{Hg}^{2+}$            | —                            | 0.5 $\mu\text{M}$          | Tap and river    | 110  |
| AgNPs-Cys                             | Filter paper          | Smartphone/RGB         | $\text{S}^{2-}$             | 0.4–4.8 $\mu\text{M}$        | 28 nM                      | Tap and seawater | 111  |
| AgNPs                                 | Filter paper          | Smartphone/RGB         | $\text{Cl}^-$               | 10–1000 mg L <sup>-1</sup>   | 1.3 mg L <sup>-1</sup>     | Natural water    | 112  |
| AgNPs-carrageenan                     | Filter paper          | Digital photometry/RGB | $\text{Hg}^{2+}$            | 0.5–2.5 mM                   | 0.29 mM                    | Water            | 113  |
| AuNPs                                 | Filter paper          | Smartphone/RGB         | $\text{Hg}^{2+}$            | 0–2 $\mu\text{M}$            | 50 nM                      | Drinking water   | 114  |
| AuNPs-Cyst                            | Filter paper          | Smartphone/RGB         | $\text{CN}^-$               | —                            | 159 nM                     | Drinking water   | 115  |
| AuNPs-hydrogel nanzyme                | Filter paper          | Smartphone/RGB         | $\text{Hg}^{2+}$            | 0.008–20 mg L <sup>-1</sup>  | 1.10 $\mu\text{g L}^{-1}$  | River water      | 116  |
| AuNPs-maleic acid                     | Filter paper          | Smartphone/RGB         | $\text{Cr}^{3+}$            | 0.2–2.0 $\mu\text{g L}^{-1}$ | 0.1 $\mu\text{g L}^{-1}$   | Lake water       | 117  |
| Nitrite + h <i>p</i> -sulfanilic acid | Solution              | Smartphone/RGB         | Triclosan                   | 3–200 $\mu\text{g L}^{-1}$   | 0.8 $\mu\text{g L}^{-1}$   | Water            | 118  |
| Molybdenum blue-PVA                   | Solution              | Smartphone/RGB         | $\text{NO}_2^-$             | 0.1–1 mg L <sup>-1</sup>     | 0.02 mg L <sup>-1</sup>    | Drinking water   | 119  |
| Molybdenum blue-PVA                   | Solution              | Smartphone/RGB         | $\text{NO}_3^-$             | 0.1–1 mg L <sup>-1</sup>     | 0.04 mg L <sup>-1</sup>    | Drinking water   | 119  |
| Molybdenum blue-PVA                   | Solution              | Smartphone/RGB         | $\text{PO}_4^{2-}$          | 0.25–5 mg L <sup>-1</sup>    | 0.14 mg L <sup>-1</sup>    | Drinking water   | 119  |
| Azophenol dye                         | Filter paper          | Smartphone/RGB         | $\text{Hg}^{2+}$            | 0–10 $\mu\text{M}$           | 8.1 nM                     | Water            | 137  |

chemometric techniques for sensor design and measurement. In the study of Fu *et al.*,<sup>123</sup> they developed an affordable portable smartphone-based hemoglobin (Hb) analyzer for point-of-care anemia testing. This device utilized a finger-prick blood sample and the smartphone's ambient light sensor to measure Hb absorptivity in a microcuvette, with the results validated by an Android-based application. The Hb analyzer demonstrated high sensitivity (95.4% for venous blood and 96.39% for fingertip blood) and selectivity (96.3% for venous blood and 95.58% for fingertip blood). It effectively diagnosed anemia in high-risk populations, including tumor chemotherapy patients, pregnant women, and thalassemia patients, and proved suitable for home-based self-testing. Luo and co-workers<sup>124</sup> introduced a cost-effective smartphone colorimeter with multi-wavelength reader for analyses of several analytes. This device used six LEDs emitting different wavelengths. It successfully detected six common serum analytes: potassium, chloride, alkaline phosphatase, alanine aminotransaminase, albumin, and glycated serum protein. This device demonstrated strong linearity ( $R^2 > 0.99$ ) across a wide range and achieved low LOD for all analytes. The results demonstrated notable accuracy, stability, and repeatability of the fabricated

device, showcasing excellent consistency with a professional microplate reader.

The body's regulation of sodium ( $\text{Na}^+$ ) is of most importance, necessitating regular monitoring. To address this need, Chandran and team<sup>68</sup> developed an affordable paper strip to measure  $\text{Na}^+$  levels in blood and urine samples. The method involves immersing paper in yellow NPs, allowing it to dry, and introducing  $\text{Na}^+$  for visual color changes. It works for a broad  $\text{Na}^+$  range (20 to 250 mM) with a low LOD of 65  $\mu\text{M}$ . Inamori and group<sup>77</sup> reported an affordable wearable bilirubinometer for neonatal jaundice monitoring. This device also simultaneously measures the heart rate and oxygen saturation, providing comprehensive vital sign monitoring. Tested on 50 newborns undergoing phototherapy, it shows promise in aiding therapeutic decisions. Wang and colleagues<sup>36</sup> presented an innovative self-healing adhesive hydrogel patch, which is assisted by a smartphone, for real-time colorimetric sweat detection. This patch, tailored for individual users, adheres securely to the skin, enabling the collection and analysis of sweat. Table 2 summarizes the applications of portable colorimetric sensing devices for the measurement of a variety of several chemical substances from clinical samples.

**Table 2** Overview of the environmental uses of portable colorimetric sensors for analyzing various chemical species in clinical samples

| Materials/probe                         | Substrate          | Sensing method       | Analyte                       | Linearity range                | LOD                         | Sample            | Ref. |
|---|--------------------|----------------------|-------------------------------|--------------------------------|-----------------------------|-------------------|------|
| AuNPs- $\beta$ -CD                      | Solution           | Smartphone/RGB       | Cysteine                      | 0.25–4.0 $\mu$ M               | 25.5 nM                     | Clinical sample   | 58   |
| CuNPs-curcumin                          | Filter paper       | Smartphone/RGB       | Na <sup>+</sup>               | 20–250 mM                      | 65 $\mu$ M                  | Serum and urine   | 68   |
| CuNPs-MSA                               | Solution           | Handheld colorimeter | Uric acid                     | 5 $\mu$ M–4.5 mM               | 3.7 $\mu$ M                 | Urine             | 69   |
| CuNPs-MSA                               | Solution           | Handheld colorimeter | H <sub>2</sub> O <sub>2</sub> | 5–500 mM                       | 4.3 $\mu$ M                 | Urine             | 69   |
| CuO-Maca                                | Filter paper       | Smartphone/RGB       | Dopamine                      | 0.625–5 $\mu$ M                | 16.9 nM                     | Clinical          | 70   |
| AuNPs                                   | Transparency sheet | Smartphone/RGB       | Vitamin B1                    | 40–200 $\mu$ g L <sup>-1</sup> | 3.0 $\mu$ g L <sup>-1</sup> | Urine             | 55   |
| MoS <sub>2</sub> /PDA/CoCu              | Solution           | Smartphone/RGB       | Uric acid                     | 0.5–200 $\mu$ M                | 0.13 $\mu$ M                | Serum and urine   | 72   |
| CuO@rGO                                 | Filter paper       | Smartphone/RGB       | Glucose                       | 1–10 mM                        | 7.0–8.0 $\mu$ M             | Human blood       | 121  |
| AuNP@PVA@MO                             | Solution           | Smartphone/RGB       | H <sub>2</sub> O <sub>2</sub> | —                              | 1.70 mM                     | Biological sample | 122  |
| 8-Hydroxy quinoline and sulfanilic acid | Solution           | Smartphone/RGB       | Atenolol                      | 8.0–60.0 mg L <sup>-1</sup>    | 2.13 mg L <sup>-1</sup>     | Pharmaceuticals   | 125  |

The advent of portable colorimetric sensing has revolutionized point-of-care diagnostics, offering swift and cost-efficient analyses. Examples include smartphone-based Hb analyzers and multi-wavelength smartphone colorimetric readers, showcasing their accuracy and potential in healthcare. Additionally, innovations like paper strips for sodium monitoring, nonenzymatic dopamine sensing, wearable bilirubinometers, and self-healing adhesive hydrogel patches for sweat analysis demonstrate the versatility and promise of colorimetric technology in enhancing healthcare diagnostics and monitoring.

### 5.3 Food safety applications

Portable colorimetric sensing plays a vital role in upholding food safety through its capability to provide real-time detection of contaminants, allergens, and indications of spoilage. Utilizing nanomaterials and smartphone-based technologies,

rapid on-site screening empowers food producers and inspectors to identify potential risks, prevent outbreaks, and maintain high food safety standards. For instance, Guembe-Garcia<sup>126</sup> developed a smartphone-assisted paper-based colorimetric sensing device for detecting NO<sub>2</sub><sup>-</sup> in processed meat. A polymeric sensor (POLYSEN) was prepared using different types of polymers, which was then placed in contact with the meat sample for 15 min in a basic medium. The color change of POLYSEN corresponded to the NO<sub>2</sub><sup>-</sup> ion concentration in the meat, and the 'colorimetric titration' application on a smartphone was used to analyze the color change, as shown in Fig. 12.

Silva and Rocha<sup>127</sup> introduced a colorimetric sensing approach to determine adulterated protein in milk. Copper sulfate was added to the milk sample to precipitate protein, and then EDTA was added to react with the remaining copper sulfate, forming a blue-colored Cu-EDTA complex. The color

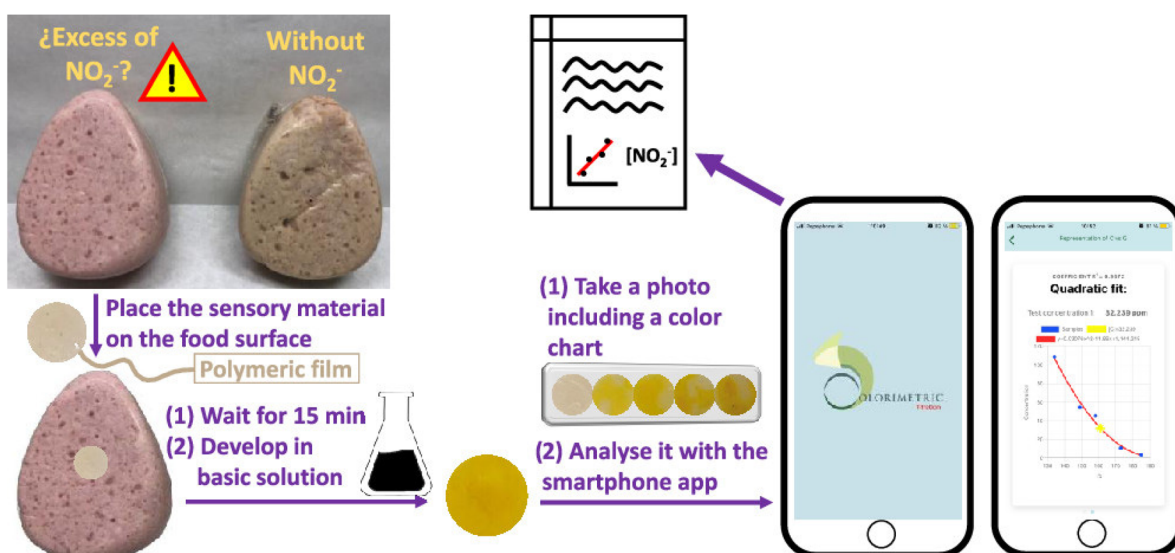


**Fig. 12** Smartphone-based colorimetric determination of the nitrite ion in a meat sample [reprinted from ref. 40 with permission from American Chemical Society].

of the complex was captured using a smartphone, and the RGB value was analyzed. The intensity of the blue-colored complex was inversely proportional to the level of adulterated protein in the milk. Lima and Coworkers<sup>128</sup> presented a method to detect the presence of  $\text{H}_2\text{O}_2$  as an adulterant in milk. This method involved adding iron(II) sulfate and potassium thiocyanate solution to the milk sample, leading to the oxidation of  $\text{Fe}^{2+}$  to  $\text{Fe}^{3+}$  in the presence of an oxidizing agent  $\text{H}_2\text{O}_2$ . The development of a red-colored iron(III) thiocyanate complex was quantified by analyzing the RGB values of a smartphone, thereby confirming the existence of  $\text{H}_2\text{O}_2$  in the milk sample. Zhang *et al.*<sup>129</sup> determined the presence of urea in milk using a smartphone-based portable colorimetric sensor. Prussian blue nanoparticles (PBNPs) and urease enzyme were added to the milk sample, resulting in the conversion of urea to  $\text{CO}_2$  and  $\text{NH}_3$  in the presence of urease, causing a change in the solution's pH. PBNPs are pH-sensitive NPs that change color with pH variation, and the smartphone captured the color change, allowing the calculation of the RGB value to assess the presence of urea in the milk sample. Liu *et al.*<sup>130</sup> developed a smartphone-based portable colorimetric sensor for  $\text{NO}_2^-$  sensing in food, based on a hydrogel microsphere substrate. Herein, *N*-(1-naphthyl) ethylenediamine was mixed with sodium alginate and further a microsphere was formed between  $\text{Ca}^{2+}$  and sodium alginate due to the strong chelation process. This microsphere shows high sensing pro-

perties of  $\text{NO}_2^-$  ions. Pickles and sausages just needed to be simply homogenized before measurements, whilst water and milk samples could be measured directly without any prior preparation. Gao and colleague<sup>131</sup> developed a paper-based colorimetric sensor based on citrate-capped AuNPs for the melamine determination in milk samples. Herein, citrate-capped AuNPs were stabilized using Triton X-100, protecting them from high ionic strength and pH range. However, melamine produced aggregation and destabilization, which resulted in a color shift from red wine to blue. A paper-based colorimetric quantitative detection system was coupled with a smartphone. This colorimetric sensor to successfully identify melamine in a milk sample in the 0.75–1.75  $\mu\text{M}$  linear range and with 5.1 nM LOD value. Chaisiwamongkhon *et al.*<sup>132</sup> designed a smartphone-coupled paper-based colorimetric sensor for the determination of sibutramine adulterants in food supplements. Herein, citrate-capped AuNPs have been used as a sensing probe for sibutramine analysis. The approach has a LOD and LOQ of 1.15 M and 3.47 M, respectively, with an accuracy of 92–107%. The technique can be used to detect and measure chemicals that have been misused instead of highly technical instruments. Sangsin and co-workers<sup>133</sup> developed a smartphone-assisted paper-based colorimetric sensor for the detection of  $\text{Cr}^{3+}$  in food samples. Herein AgNPs were used as a functionalized material and deposited on a paper substrate for on-site monitoring of  $\text{Cr}^{3+}$ . A

**Table 3** Overview of the environmental uses of portable colorimetric sensors for analyzing various chemical species in food samples

| Materials/probe                              | Substrate         | Sensing method     | Analyte                | Linearity range               | LOD                     | Sample                | Ref. |
|--|-------------------|--------------------|------------------------|-------------------------------|-------------------------|-----------------------|------|
| 4'-Hydroxyl-2,4-diaminoazobenzene            | Paper             | Smartphone/RGB     | $\text{Al}^{3+}$       | 20 $\mu\text{M}$ –2.0 mM      | 2.36 $\mu\text{M}$      | Food and toothpaste   | 47   |
| 4'-Hydroxyl-2,4-diaminoazobenzene            | Paper             | Smartphone/RGB     | $\text{Fe}^{3+}$       | 20 $\mu\text{M}$ –2.0 mM      | 2.68 $\mu\text{M}$      | Food and toothpaste   | 47   |
| CuONPs- <i>Camellia sinensis</i> polyphenols | Filter paper      | Smartphone/RGB     | $\text{NH}_3$          | 12.5–100 $\mu\text{M}$        | 40.6 nM                 | Food supplements      | 71   |
| Cu@Ag NPs                                    | Filter paper      | Smartphone/RGB     | Dimethoate             | 100–2000 $\mu\text{g L}^{-1}$ | 30 $\mu\text{g L}^{-1}$ | Food                  | 73   |
| Fe-SAN                                       | Solution          | Smartphone/RGB     | Ascorbic acid          | 0.5–100 $\mu\text{M}$         | 0.315 $\mu\text{M}$     | Tropical fruits       | 86   |
| 1,2-Naphthoquinone-4-sulfonate               | Wax printed paper | Computer/RGB       | Phenacetin             | 0–64.52 mg $\text{L}^{-1}$    | 3.5 mg $\text{L}^{-1}$  | Seized cocaine sample | 92   |
| AgNPs-carrageenan                            | Filter paper      | Digital photometry | $\text{Hg}^{2+}$       | —                             | 292 $\mu\text{M}$       | Environmental sample  | 113  |
| Polymer                                      | Filter paper      | Smartphone/RGB     | $\text{NO}_2^-$        | 1–300                         | 0.85 mg $\text{L}^{-1}$ | Meat                  | 126  |
| Prussian blue NPs                            | Filter paper      | Smartphone/RGB     | Urea                   | 0.5–5 mM                      | 0.27 mM                 | Milk                  | 129  |
| AuNPs-Triton X100                            | Filter paper      | Smartphone/RGB     | Melamine               | 0.75–1.75 $\mu\text{M}$       | 5.1 nM                  | Milk                  | 131  |
| AuNPs  | Filter paper      | Smartphone/RGB     | Sibutramine            | 5–15 $\mu\text{M}$            | 3.47 $\mu\text{M}$      | Food supplements      | 132  |
| AgNPs  | Filter paper      | Smartphone/RGB     | $\text{Cr}^{3+}$       | 2–5 mg $\text{L}^{-1}$        | 1.52 mg $\text{L}^{-1}$ | Dietary supplement    | 133  |
| AgNPs- <i>Lepidium meyenii</i> polyphenols   | Filter paper      | Smartphone/RGB     | $\text{H}_2\text{O}_2$ | 0.5–5000 $\mu\text{M}$        | 3.84 $\mu\text{M}$      | Milk                  | 134  |
| AgNPs  | Filter paper      | Smartphone/RGB     | $\text{H}_2\text{O}_2$ | 0.1–10 mM                     | 0.1 mM                  | Food supplement       | 135  |
| AgNPs-metronidazole                          | Filter paper      | Smartphone/RGB     | Permethrin             | —                             | 0.010 $\mu\text{M}$     | Tomato and apple      | 136  |
| AgNPs-green dendrimer-coated matcha extract  | Filter paper      | Smartphone/RGB     | $\text{H}_2\text{O}_2$ | 0.05–20 $\mu\text{M}$         | 0.82 $\mu\text{M}$      | Food supplement       | 137  |

smartphone readout system was used to create a low-cost portable way to detect  $\text{Cr}^{3+}$ . In a short period of time, the system monitors color intensities in the AgNP system. The system is very selective with a linear range of  $2.0\text{--}5.0 \text{ mg L}^{-1}$ , and  $1.52 \text{ mg L}^{-1}$  of LOD; it has been successfully employed for dietary supplement quantification, demonstrating practicality and reproducibility for on-site  $\text{Cr}^{3+}$  detection in real samples. A paper-based food safety process using different sensing probes such as NMs and dyes<sup>134–137</sup> ensures quality checks, tracks contamination, and educates users, enhancing the overall food safety through accessible, cost-effective, and efficient methods. Table 3 summarizes the applications of portable colorimetric sensing devices for the measurement of a variety of several chemical substances from food samples.

Therefore, portable colorimetric sensing is vital for ensuring food safety by enabling real-time detection of pollutants, allergens, and spoilage indicators. Utilizing nanomaterials and chromophoric reagents assisted with smartphone-based systems, it empowers food professionals to swiftly identify risks, maintain safety standards, and educate consumers. A range of smartphone-assisted colorimetric devices have been developed for detecting various food contaminants, offering accessible, cost-effective, and efficient methods to enhance food safety and public health.

## 6. Conclusion

In conclusion, this review article on portable colorimetric sensing applications has given an in-depth overview of the key developments and a wide variety of uses in this rapidly growing topic. The combination of portable devices and colorimetric sensing has developed several industries, including healthcare, environmental monitoring, food safety, and industrial quality control. The review emphasizes how these portable sensing systems are adaptable, sensitive, and straightforward, which makes them attractive for on-site real-time analysis.

The surprising innovation in nanomaterials and chromophoric dyes has improved the sensitivity and selectivity of portable colorimetric sensors. The use of label-free and signal amplification methods, which have enhanced detection limits and increased analyte selectivity, has been made possible by the use of nanomaterials such as nanoparticles, quantum dots, and nanostructured materials. In addition, the development of mobile sensing devices like smartphones and paper-based systems has opened up access to analytical data. On-the-go and point-of-care diagnostics are now possible because of the accessibility and affordability of cell phones, especially in resource-constrained areas where access to conventional laboratory facilities is constrained. Paper-based detecting systems offer an ecologically safe and cost-effective substitute for rapid detection, especially in remote areas or during emergencies.

## Conflicts of interest

There are no conflicts to declare.

## References

- 1 K. Lebelo, N. Malebo, M. J. Mochane and M. Masinde, *Int. J. Environ. Res. Public Health*, 2021, **18**, 5795.
- 2 J. F. Hernández-Rodríguez, D. Rojas and A. Escarpa, *Anal. Chem.*, 2021, **93**, 167–183.
- 3 J. E. Casida and K. A. Durkin, *Chem. Res. Toxicol.*, 2017, **30**, 94–104.
- 4 G. Tmušić, S. Manfreda, H. Aasen, M. R. James, G. Gonçalves, E. Ben-Dor, A. Brook, M. Polinova, J. J. Arranz, J. Mészáros, R. Zhuang, K. Johansen, Y. Malbeteau, I. P. de Lima, C. Davids, S. Herban and M. F. McCabe, *Remote Sens.*, 2020, **12**, 1001.
- 5 N. Panwar, A. M. Soehartono, K. K. Chan, S. Zeng, G. Xu, J. Qu, P. Coquet, K.-T. Yong and X. Chen, *Chem. Rev.*, 2019, **119**, 9559–9656.
- 6 B. Kartoglu, A. Bahçivan, S. Erarpat, A. Bayraktar and S. Bakirdere, *J. Food Compos. Anal.*, 2023, **121**, 105373.
- 7 J. Mrmošanin, A. Pavlović, I. Rašić Mišić, S. Tošić, S. Petrović, Z. Mitić, E. Pecev-Marinković and B. Arsić, *Anal. Lett.*, 2023, 1–14.
- 8 V. Balaram, L. Copia, U. S. Kumar, J. Miller and S. Chidambaram, *GeoGeo*, 2023, **2**, 100210.
- 9 S. Patel, K. Shrivats, D. Sinha, I. Karbhal, T. K. Patle, Monisha and Tikeshwari, *Spectrochim. Acta, Part A*, 2023, **299**, 122824.
- 10 T. Kant, K. Shrivats and V. Ganesan, *RSC Adv.*, 2023, **13**, 17179–17187.
- 11 P. Kassal, M. D. Steinberg, E. Horak and I. M. Steinberg, *Sens. Actuators, B*, 2018, **275**, 230–236.
- 12 T. Kant, K. Shrivats, K. Dewangan, A. Kumar, N. K. Jaiswal, M. K. Deb and S. Pervez, *Mater. Today Chem.*, 2022, **24**, 100769.
- 13 T. Kumar Patle, K. Shrivats, A. Patle, S. Patel, N. Harmukh and A. Kumar, *Microchem. J.*, 2022, **176**, 107249.
- 14 A. Garg, M. Akbar, E. Vejerano, S. Narayanan, L. Nazhandali, L. C. Marr and M. Agah, *Sens. Actuators, B*, 2015, **212**, 145–154.
- 15 A. de Villiers, P. Venter and H. Pasch, *J. Chromatogr. A*, 2016, **1430**, 16–78.
- 16 L. G. Johnsen, P. B. Skou, B. Khakimov and R. Bro, *J. Chromatogr. A*, 2017, **1503**, 57–64.
- 17 S. Patel, R. Jamunkar, D. Sinha, Monisha, T. K. Patle, T. Kant, K. Dewangan and K. Shrivats, *Trends Environ. Anal. Chem.*, 2021, **31**, e00136.
- 18 S. Sahu, S. Sharma, T. Kant, K. Shrivats and K. K. Ghosh, *Spectrochim. Acta, Part A*, 2021, **246**, 118961.
- 19 K. Shrivats, W. Naik, D. Kumar, D. Singh, K. Dewangan, T. Kant, S. Yadav, Tikeshwari and N. Jaiswal, *Microchem. J.*, 2021, **160**, 105597.
- 20 X. Jia, P. Ma, K. Tarwa and Q. Wang, *J. Agric. Food Res.*, 2023, **11**, 100503.
- 21 W. Tan, L. Zhang, P. Jarujamrus, J. C. G. Doery and W. Shen, *Microchem. J.*, 2022, **180**, 107562.
- 22 S. J. Oh, B. H. Park, G. Choi, J. H. Seo, J. H. Jung, J. S. Choi, D. H. Kim and T. S. Seo, *Lab Chip*, 2016, **16**, 1917–1926.

23 K. Shrivats, R. Shankar and K. Dewangan, *Sens. Actuators, B*, 2015, **220**, 1376–1383.

24 K. Shrivats, N. Nirmalkar, S. S. Thakur, M. K. Deb, S. S. Shinde and R. Shankar, *Food Chem.*, 2018, **250**, 14–21.

25 K. Shrivats, S. Sahu, B. Sahu, R. Kurrey, T. K. Patle, T. Kant, I. Karbhal, M. L. Satnami, M. K. Deb and K. K. Ghosh, *J. Mol. Liq.*, 2019, **275**, 297–303.

26 W. Wang, Y. You and S. Gunasekaran, *Compr. Rev. Food Sci. Food Saf.*, 2021, **20**, 5829–5855.

27 D. Kim, S. Kim, H.-T. Ha and S. Kim, *Curr. Appl. Phys.*, 2020, **20**, 1013–1018.

28 A. Koh, D. Kang, Y. Xue, S. Lee, R. M. Pielak, J. Kim, T. Hwang, S. Min, A. Banks, P. Bastien, M. C. Manco, L. Wang, K. R. Ammann, K.-I. Jang, P. Won, S. Han, R. Ghaffari, U. Paik, M. J. Slepian, G. Balooch, Y. Huang and J. A. Rogers, *Sci. Transl. Med.*, 2016, **8**, 366ra165–366ra165.

29 H. Shi, Y. Cao, Y. Zeng, Y. Zhou, W. Wen, C. Zhang, Y. Zhao and Z. Chen, *Talanta*, 2022, **240**, 123208.

30 W. Kurz, A. K. Yetisen, M. V. Kaito, M. J. Fuchter, M. Jakobi, M. Elsner and A. W. Koch, *Adv. Opt. Mater.*, 2020, **8**, 1901969.

31 F. Liu, J.-L. Han, J. Qi, Y. Zhang, J.-L. Yu, W.-P. Li, D. Lin, L.-X. Chen and B.-W. Li, *Chin. J. Anal. Chem.*, 2021, **49**, 159–171.

32 V. Oncescu, D. O'Dell and D. Erickson, *Lab Chip*, 2013, **13**, 3232–3238.

33 H. Shi, Y. Cao, Z. Xie, Y. Zhao, C. Zhang and Z. Chen, *Sens. Actuators, B*, 2022, **372**, 132644.

34 N. Promphet, S. Ummartyotin, W. Ngeontae, P. Puthongkham and N. Rodthongkum, *Anal. Chim. Acta*, 2021, **1179**, 338643.

35 B. Purohit, A. Kumar, K. Mahato and P. Chandra, *Curr. Opin. Biomed. Eng.*, 2020, **13**, 42–50.

36 L. Wang, T. Xu, X. He and X. Zhang, *J. Mater. Chem. C*, 2021, **9**, 14938–14945.

37 K. Laganovska, A. Zolotarjovs, M. Vázquez, K. Mc Donnell, J. Liepins, H. Ben-Yoav, V. Karitans and K. Smits, *HardwareX*, 2020, **7**, e00108.

38 S. Mukherjee, M. Shah, K. Chaudhari, A. Jana, C. Sudhakar, P. Srikrishnarka, M. R. Islam, L. Philip and T. Pradeep, *ACS Omega*, 2020, **5**, 25253–25263.

39 M. S. Braga, R. F. V. V. Jaimes, W. Borysow, O. F. Gomes and W. J. Salcedo, *Sensors*, 2017, **1730**, 17.

40 A. Shahvar, D. Shamsaei and M. Saraji, *Measurement*, 2020, **150**, 107068.

41 S. Dutta, G. P. Saikia, D. J. Sarma, K. Gupta, P. Das and P. Nath, *J. Biophotonics*, 2017, **10**, 623–633.

42 T. Alawsi, G. P. Mattia, Z. Al-Bawi and R. Beraldí, *Sens. Bio-Sens. Res.*, 2021, **32**, 100404.

43 S. Sajed, M. Kolahdouz, M. A. Sadeghi and S. F. Razavi, *ACS Omega*, 2020, **5**, 27675–27684.

44 K. Shrivats, Monisha, T. Kant, I. Karbhal, R. Kurrey, B. Sahu, D. Sinha, G. K. Patra, M. K. Deb and S. Pervez, *Anal. Bioanal. Chem.*, 2020, **412**, 1573–1583.

45 E. Celikbas, A. E. Ceylan and S. Timur, *Talanta*, 2020, **208**, 120446.

46 X. Bao, S. Jiang, Y. Wang, M. Yu and J. Han, *Analyst*, 2018, **143**, 1387–1395.

47 H. Ren, F. Li, S. Yu and P. Wu, *Heliyon*, 2022, **8**, e10216.

48 Ranbir, G. Singh, H. Singh, N. Kaur and N. Singh, *Sens. Actuators, B*, 2023, **387**, 133794.

49 K. Vellingiri, V. Choudhary and L. Philip, *J. Environ. Chem. Eng.*, 2019, **7**, 103374.

50 Y. Chen, G. Fu, Y. Zilberman, W. Ruan, S. K. Ameri, Y. S. Zhang, E. Miller and S. R. Sonkusale, *Food Control*, 2017, **82**, 227–232.

51 X. Liu, D. Huo, J. Li, Y. Ma, H. Liu, H. Luo, S. Zhang, X. Luo and C. Hou, *Food Chem.*, 2023, **415**, 135525.

52 L. Yu, Z. Song, J. Peng, M. Yang, H. Zhi and H. He, *TrAC, Trends Anal. Chem.*, 2020, **127**, 115880.

53 H. H. Cho, J. H. Heo, D. H. Jung, S. H. Kim, S.-J. Suh, K. H. Han and J. H. Lee, *BioChip J.*, 2021, **15**, 276–286.

54 L. Zhang, D. Huang, P. Zhao, G. Yue, L. Yang and W. Dan, *Spectrochim. Acta, Part A*, 2022, **269**, 120748.

55 P. Duenchay, K. Kaewjua, O. Chailapakul and W. Siangproh, *New J. Chem.*, 2020, **44**, 9223–9229.

56 Y. Gan, T. Liang, Q. Hu, L. Zhong, X. Wang, H. Wan and P. Wang, *Talanta*, 2020, **208**, 120231.

57 A. R. Esfahani, Z. Sadiq, O. D. Oyewunmi, S. H. Safiabadi Tali, N. Usen, D. C. Boffito and S. Jahanshahi-Anbuhi, *Analyst*, 2021, **146**, 3697–3708.

58 R. Rajamanikandan, A. D. Lakshmi and M. Ilanchelian, *New J. Chem.*, 2020, **44**, 12169–12177.

59 S. Sahu, S. Sharma, R. Kurrey and K. K. Ghosh, *Environ. Sci. Nano*, 2022, **9**, 3684–3710.

60 Monisha, K. Shrivats, T. Kant, S. Patel, R. Devi, N. S. Dahariya, S. Pervez, M. K. Deb, M. K. Rai and J. Rai, *J. Hazard. Mater.*, 2021, **414**, 125440.

61 K. Shrivats, B. Sahu, M. K. Deb, S. S. Thakur, S. Sahu, R. Kurrey, T. Kant, T. K. Patle and R. Jangde, *Microchem. J.*, 2019, **150**, 104156.

62 T. Kant, K. Shrivats, V. Ganesan, Y. K. Mahipal, R. Devi, M. K. Deb and R. Shankar, *Microchem. J.*, 2020, **155**, 104687.

63 M. Mavaei, A. Chahardoli, A. Fattahi and A. Khoshroo, *Global Challenges*, 2021, **5**, 2000099.

64 J. Infant, T. Ebenezer, R. R. Gopi, H. Joy Prabu, I. Johnson and A. Joseph Anthuvan, *Mater. Today: Proc.*, 2022, **68**, 319–325.

65 A. W. Kahandal, L. Sharma, V. Sirdeshmukh, A. Kulkarni and C. K. Tagad, *Int. J. Environ. Sci. Technol.*, 2023, **20**, 9077–9088.

66 F. Zarif, S. Khurshid, N. Muhammad, M. Zahid Qureshi and N. S. Shah, *ChemistrySelect*, 2020, **5**, 6066–6074.

67 R. A. Soomro, A. Nafady, Sirajuddin, N. Memon, T. H. Sherazi and N. H. Kalwar, *Talanta*, 2014, **130**, 415–422.

68 N. Chandran, P. Janardhanan, M. Bayal, R. Pilankatta and S. S. Nair, *Sci. Rep.*, 2022, **12**, 1–15.

69 C. Ma, L. Kong, X. Sun, Y. Zhang, X. Wang, X. Wei, H. Wan and P. Wang, *Talanta*, 2023, **255**, 124196.

70 M. İlgar, G. Baytemir, N. Taşaltın, S. Güllülü, İ. S. Yeşilyurt and S. Karakuş, *J. Photochem. Photobiol. A*, 2022, **431**, 114075.

71 S. Karakuş, G. Baytemir, C. Özeroğlu and N. Taşaltın, *Inorg. Chem. Commun.*, 2022, **143**, 109733.

72 J. Chen, X. Wang, Y. Wang, Y. Zhang, Z. Peng, X. Tang, Y. Hu and P. Qiu, *Microchem. J.*, 2023, **189**, 108541.

73 S. Patel, K. Shrivastava, D. Sinha, Monisha, T. Kumar Patle, S. Yadav, S. S. Thakur, M. K. Deb and S. Pervez, *Food Chem.*, 2022, **383**, 132449.

74 Y. Zhang, Q. Luo, K. Ding, S. G. Liu and X. Shi, *Sens. Actuators, B*, 2021, **335**, 129708.

75 M. M. Bordbar, J. Tashkhourian and B. Hemmateenejad, *ACS Appl. Mater. Interfaces*, 2022, **14**, 8333–8342.

76 S. Srivastava and V. Sharma, *Appl. Water Sci.*, 2021, **11**, 177.

77 G. Inamori, U. Kamoto, F. Nakamura, Y. Isoda, A. Uozumi, R. Matsuda, M. Shimamura, Y. Okubo, S. Ito and H. Ota, *Sci. Adv.*, 2021, **7**, eabe3793.

78 R. Kumar, P. Rauwel, M. Kriipsalu and E. Rauwel, *J. Phys.: Conf. Ser.*, 2022, **2315**, 012031.

79 Z. Yu, R. Meng, S. Deng and L. Jia, *Spectrochim. Acta, Part A*, 2023, **287**, 122072.

80 S. Šafranko, P. Živković, A. Stanković, M. Medvidović-Kosanović, A. Széchenyi and S. Jokić, *J. Chem. Educ.*, 2019, **96**, 1928–1937.

81 R. Rajamanikandan, M. Ilanchelian and H. Ju, *Chemosphere*, 2023, **340**, 139838.

82 K. Shrivastava, S. Patel, D. Sinha, S. S. Thakur, T. K. Patle, T. Kant, K. Dewangan, M. L. Satnami, J. Nirmalkar and S. Kumar, *Microchim. Acta*, 2020, **187**, 173.

83 C. Dong, X. Ma, N. Qiu, Y. Zhang and A. Wu, *Sens. Actuators, B*, 2021, **329**, 129066.

84 X. Wang, T.-W. Chang, G. Lin, M. R. Gartia and G. L. Liu, *Anal. Chem.*, 2017, **89**, 611–615.

85 C. Dong, Z. Wang, Y. Zhang, X. Ma, M. Z. Iqbal, L. Miao, Z. Zhou, Z. Shen and A. Wu, *ACS Sens.*, 2017, **2**, 1152–1159.

86 Y. Li, R. Javed, R. Li, Y. Zhang, Z. Lang, H. Zhao, X. Liu, H. Cao and D. Ye, *Food Chem.*, 2023, **406**, 135017.

87 V. Choudhary and L. Philip, *Microchem. J.*, 2021, **171**, 106809.

88 M. L. Firdaus, A. Aprian, N. Meileza, M. Hitsmi, R. Elvia, L. Rahmidar and R. Khaydarov, *Chemosensors*, 2019, **7**, 25.

89 J. Zhu, X. Yin, W. Zhang, M. Chen, D. Feng, Y. Zhao and Y. Zhu, *Biosensors*, 2023, **13**, 309.

90 Q. Kong, Y. Wang, L. Zhang, S. Ge and J. Yu, *Sens. Actuators, B*, 2017, **243**, 130–136.

91 N. Ratnarathorn, O. Chailapakul, C. S. Henry and W. Dungchai, *Talanta*, 2012, **99**, 552–557.

92 G. O. da Silva, W. R. de Araujo and T. R. L. C. Paixão, *Talanta*, 2018, **176**, 674–678.

93 W.-Y. Zhang, H. Zhang and F.-Q. Yang, *Chemosensors*, 2022, **10**, 335.

94 J.-f. Guo, D.-q. Huo, M. Yang, C.-j. Hou, J.-j. Li, H.-b. Fa, H.-b. Luo and P. Yang, *Talanta*, 2016, **161**, 819–825.

95 J. Xiao, Y. Liu, L. Su, D. Zhao, L. Zhao and X. Zhang, *Anal. Chem.*, 2019, **91**, 14803–14807.

96 M. Finnegan, E. Duffy and A. Morrin, *Sens. Bio-Sens. Res.*, 2022, **35**, 100473.

97 S.-H. Hwang, Y. K. Kim, S. M. Jeong, C. Choi, K. Y. Son, S.-K. Lee and S. K. Lim, *Text. Res. J.*, 2020, **90**, 2198–2211.

98 J.-H. Ha, Y. Jeong, J. Ahn, S. Hwang, S. Jeon, D. Kim, J. Ko, B. Kang, Y. Jung, J. Choi, H. Han, J. Gu, S. Cho, H. Kim, M. Bok, S. A. Park, J.-H. Jeong and I. Park, *Mater. Horiz.*, 2023, **10**, 4163–4171.

99 X.-Q. You, Q.-Y. He, T.-W. Wu, D.-Y. Huang, Z.-Z. Peng, D.-Y. Chen, Z. Chen and J. Liu, *Microchem. J.*, 2023, **190**, 108570.

100 K. Zhang, J. Zhang, F. Wang and D. Kong, *ACS Sens.*, 2021, **6**, 2261–2269.

101 Z. Chen, L. Chen, L. Lin, Y. Wu and F. Fu, *ACS Sens.*, 2018, **3**, 2145–2151.

102 A. Vaquer, E. Barón and R. de la Rica, *ACS Sens.*, 2021, **6**, 130–136.

103 X. He, T. Xu, Z. Gu, W. Gao, L.-P. Xu, T. Pan and X. Zhang, *Anal. Chem.*, 2019, **91**, 4296–4300.

104 T. Xu, W. Shi, J. Huang, Y. Song, F. Zhang, L.-P. Xu, X. Zhang and S. Wang, *ACS Nano*, 2017, **11**, 621–626.

105 T. Wu, T. Xu, L.-P. Xu, Y. Huang, W. Shi, Y. Wen and X. Zhang, *Biosens. Bioelectron.*, 2016, **86**, 951–957.

106 M. Sargazi and M. Kaykhaii, *Spectrochim. Acta, Part A*, 2020, **227**, 117672.

107 H. Li, T. Fang, Q.-G. Tan and J. Ma, *Sci. Total Environ.*, 2022, **838**, 156197.

108 Y. Cao, Y. Liu, F. Li, S. Guo, Y. Shui, H. Xue and L. Wang, *Microchem. J.*, 2019, **150**, 104176.

109 X. Liu, Z. Chen, R. Gao, C. Kan and J. Xu, *J. Environ. Chem. Eng.*, 2022, **10**, 107650.

110 M. L. Budlayan, J. Dalagan, J. P. Lagare-Oracion, J. Patricio, S. Arco, F. Latayada, T. Vales, B. Baje, A. Alguno and R. Capangpangan, *Environ. Nanotechnol., Monit. Manage.*, 2022, **18**, 100736.

111 R. Rajamanikandan and M. Ilanchelian, *Microchem. J.*, 2022, **174**, 107071.

112 A. Yakoh, P. Rattanarat, W. Siangproh and O. Chailapakul, *Talanta*, 2018, **178**, 134–140.

113 M. O. S. Lobregas, J. P. O. Bantang and D. H. Camacho, *Sens. Bio-Sens. Res.*, 2019, **26**, 100303.

114 G.-H. Chen, W.-Y. Chen, Y.-C. Yen, C.-W. Wang, H.-T. Chang and C.-F. Chen, *Anal. Chem.*, 2014, **86**, 6843–6849.

115 R. Rajamanikandan, K. Shanmugaraj, M. Ilanchelian and H. Ju, *Chemosphere*, 2023, **316**, 137836.

116 E. Ko, W. Hur, S. E. Son, G. H. Seong and D. K. Han, *Microchim. Acta*, 2021, **188**, 382.

117 H. Li, W. Dong, C. Li, T. Barakat, M. Sun, Y. Wang, L. Wu, L. Wang, L. Xia, Z.-Y. Hu, Y. Li and B.-L. Su, *J. Energy Chem.*, 2022, **68**, 624–636.

118 M. Shahvalinia, A. Larki and K. Ghanemi, *Spectrochim. Acta, Part A*, 2022, **278**, 121323.

119 W. Wongniramaikul, B. Kleangklaor, C. Boonkanon, T. Taweekarn, K. Phatthanawiwat, W. Sriprom, W. Limsakul, W. Towanlong, D. Tipmanee and A. Choodum, *Molecules*, 2022, **27**, 7287.

120 G. Singh, P. Raj, H. Singh and N. Singh, *J. Mater. Chem. C*, 2018, **6**, 12728–12738.

121 M. Srivastava, S. K. Srivastava, R. P. Ojha and R. Prakash, *Microchem. J.*, 2022, **182**, 107850.

122 K. N. O. dos Santos and M. B. Mamián-López, *Anal. Bioanal. Chem.*, 2023, **415**, 4459–4466.

123 Q. Fu, T. Qi, Z. Wu, Y. He, S. Guan, S. Luo, Q. Zhang, W. Luo, W. Xiao, B. Situ and L. Zheng, *Biosens. Bioelectron.*, 2022, **217**, 114711.

124 W. Luo, J. Deng, J. He, Z. Han, C. Huang, Y. Li, Q. Fu and H. Chen, *Sens. Actuators, B*, 2021, **329**, 129266.

125 R. O. Hassan, H. O. Othman and D. S. Ali, *Spectrochim. Acta, Part A*, 2023, **302**, 123009.

126 M. Guembe-García, L. González-Ceballos, A. Arnaiz, M. A. Fernández-Muiño, M. T. Sancho, S. M. Osés, S. Ibeas, J. Rovira, B. Melero, C. Represa, J. M. García and S. Vallejos, *ACS Appl. Mater. Interfaces*, 2022, **14**, 37051–37058.

127 A. F. S. Silva and F. R. P. Rocha, *Food Control*, 2020, **115**, 107299.

128 M. J. A. Lima, M. K. Sasaki, O. R. Marinho, T. A. Freitas, R. C. Faria, B. F. Reis and F. R. P. Rocha, *Microchem. J.*, 2020, **157**, 105042.

129 W.-Y. Zhang, C.-Y. Zhang, H.-Y. Zhou, T. Tian, H. Chen, H. Zhang and F.-Q. Yang, *Microchem. J.*, 2022, **181**, 107783.

130 S. Liu, H. Qu, L. Yao, Y. Mao, L. Yan, B. Dong and L. Zheng, *Sens. Actuators, B*, 2023, **397**, 134707.

131 N. Gao, P. Huang and F. Wu, *Spectrochim. Acta, Part A*, 2018, **192**, 174–180.

132 K. Chaisiwamongkhol, S. Labaide, S. Pon-in, S. Pinsrithong, T. Bunchuay and A. Phonchai, *Microchem. J.*, 2020, **158**, 105273.

133 S. Sangsin, P. Srivilai and P. Tongraung, *Spectrochim. Acta, Part A*, 2021, **246**, 119050.

134 S. Karakuş, G. Baytemir and N. Taşaltın, *Appl. Phys. A*, 2022, **128**, 390.

135 L. Sharma, S. Gouraj, P. Raut and C. Tagad, *Environ. Technol.*, 2021, **42**, 3441–3450.

136 S. Rasheed, M. A. ul Haq, N. Ahmad, Sirajuddin and D. Hussain, *Food Chem.*, 2023, **429**, 136925.

137 E. Tan, İ. M. Kahyaoğlu and S. Karakuş, *Polym. Bull.*, 2022, **79**, 7363–7389.